OPEN ACCESS

ORIGINAL ARTICLE

Canonical Wnt signals combined with suppressed TGFβ/BMP pathways promote renewal of the native human colonic epithelium

Amy Reynolds,[1] Natalia Wharton,[1] Alyson Parris,[1] Esther Mitchell,[1] Anastasia Sobolewski,[2] Christy Kam,[1] Loren Bigwood,[1] Ahmed El Hadi,[1] Andrea Münsterberg,[1] Michael Lewis,[3] Christopher Speakman,[3] William Stebbings,[3] Richard Wharton,[3] Kevin Sargen,[3] Richard Tighe,[4] Crawford Jamieson,[4] James Hernon,[3] Sandeep Kapur,[3] Naohide Oue,[5] Wataru Yasui,[5] Mark R Williams[1]

▶ Additional material is published online only. To view please visit the journal online (http://dx.doi.org/10.1136/gutjnl-2012-304067).

[1]School of Biological Sciences, University of East Anglia, Norwich Research Park, Norwich, Norfolk, UK
[2]Department of Gut Health and Food Safety, Institute Strategic Programme, Institute of Food Research, Colney, Norwich Research Park, Norwich, Norfolk, UK
[3]Department of Surgery, Norfolk and Norwich University Hospitals Trust, Colney Lane, Norwich Research Park, Norwich, Norfolk, UK
[4]Department of Gastroenterology, Norfolk and Norwich University Hospitals Trust, Colney Lane, Norwich Research Park, Norwich, Norfolk, UK
[5]Department of Molecular Pathology, Hiroshima University Institute of Biomedical and Health Sciences, Hiroshima, Japan

Correspondence to
Dr Mark R Williams, School of Biological Sciences, University of East Anglia, Norwich Research Park, Norwich, Norfolk NR47TJ, UK; m.r.williams@uea.ac.uk

AR, NW and AP contributed equally.

Received 5 November 2012
Revised 29 May 2013
Accepted 31 May 2013

To cite: Reynolds A, Wharton N, Parris A, *et al*. *Gut* Published Online First: [*please include* Day Month Year] doi:10.1136/gutjnl-2012-304067

ABSTRACT

Background A defining characteristic of the human intestinal epithelium is that it is the most rapidly renewing tissue in the body. However, the processes underlying tissue renewal and the mechanisms that govern their coordination have proved difficult to study in the human gut.

Objective To investigate the regulation of stem cell-driven tissue renewal by canonical Wnt and TGFβ/bone morphogenetic protein (BMP) pathways in the native human colonic epithelium.

Design Intact human colonic crypts were isolated from mucosal tissue samples and placed into 3D culture conditions optimised for steady-state tissue renewal. High affinity mRNA in situ hybridisation and immunohistochemistry were complemented by functional genomic and bioimaging techniques. The effects of signalling pathway modulators on the status of intestinal stem cell biology, crypt cell proliferation, migration, differentiation and shedding were determined.

Results Native human colonic crypts exhibited distinct activation profiles for canonical Wnt, TGFβ and BMP pathways. A population of intestinal LGR5/OLFM4-positive stem/progenitor cells were interspersed between goblet-like cells within the crypt-base. Exogenous and crypt cell-autonomous canonical Wnt signals supported homeostatic intestinal stem/progenitor cell proliferation and were antagonised by TGFβ or BMP pathway activation. Reduced Wnt stimulation impeded crypt cell proliferation, but crypt cell migration and shedding from the crypt surface were unaffected and resulted in diminished crypts.

Conclusions Steady-state tissue renewal in the native human colonic epithelium is dependent on canonical Wnt signals combined with suppressed TGFβ/BMP pathways. Stem/progenitor cell proliferation is uncoupled from crypt cell migration and shedding, and is required to constantly replenish the crypt cell population.

Significance of this study

What is already known about this subject?

- In the mouse, renewal of the intestinal epithelium is regulated by signalling cross-talk between the Wnt, Notch, epidermal growth factor (EGF) and TGFβ/BMP pathways.
- Wnt signals predominate at the intestinal crypt-base and maintain intestinal stem cell biology.
- LGR5, a Wnt target gene, is a marker for mouse intestinal stem cells.
- Wnt signals are required for the development of mouse intestinal organoids from single intestinal stem cells in culture.
- Additional pharmacological strategies have led to the development of spheroid and budding organoid systems for the long-term culture of human intestinal stem cells.

What are the new findings?

- Tissue renewal in the native human colonic epithelium can be studied in real time ex vivo.
- Wnt signals in combination with suppressed TGFβ/BMP pathways maintain the hierarchy and procession of tissue renewal along the human colonic crypt-axis.
- A population of proliferative LGR5/OLFM4-positive stem/progenitor cells are supported by Wnt signals at the crypt-base.
- We propose that crypt cell migration and shedding is the default state and that Wnt signals are required for steady-state tissue renewal.

How might it impact on clinical practice in the foreseeable future?

- The native human colonic crypt culture model will permit functional interrogation of the status and mechanisms underlying tissue renewal in the healthy ageing human colonic epithelium and in tissue at risk of disease.
- The use of native human tissue will help the development and translation of novel strategies for the prevention of cancer and inflammatory bowel disease.

INTRODUCTION

Along with other self-renewing tissues such as skin and bone marrow, the mammalian gut epithelium is one of the most dynamic tissues in the body. The constant renewal cycle is of 5–7 days duration and takes place in a hostile environment characterised by the presence of bacterial toxins and metabolites,

dietary antigens and mutagens, and immunological cytokines and oxidative stress. Approximately 10 billion cells are shed from the gut epithelium each day and these are continuously replaced by intestinal stem cell progeny. The colonic epithelium is exquisitely organised into millions of invaginations called crypts, each of which represents the self-renewing unit of the tissue. At the base of every crypt, it is thought that intestinal stem cells divide symmetrically to self-renew and undertake a progenitor phenotype on exiting the stem cell niche.[1 2] Stem cell progeny (transit amplifying cells) proliferate, migrate and differentiate (into enterocytes, goblet cells, enteroendocrine cells and tuft cells) along the crypt-axis before they are shed from the surface epithelium. The hierarchy of tissue renewal is thought to minimise the accumulation of molecular damage by virtue of positioning long-lived stem cells in a relatively safe harbour at the crypt-base, from where they fuel the constant replenishment of shed cells. The molecular mechanisms that regulate the physiological processes of tissue renewal are of the utmost interest because they are disrupted in conditions such as inflammatory bowel disease and colon cancer.

A small number of highly conserved signalling pathways that play a key role in developmental biology have also been implicated in regulating the hierarchy of intestinal tissue renewal in the adult. A series of elegant studies in the mouse have suggested that reciprocal morphogenic gradients along the crypt-axis orchestrate stem/progenitor cell proliferation, lineage specification, migration, differentiation and shedding.[3 4] The canonical Wnt signalling pathway has been deemed the master regulator of intestinal tissue renewal.[5] Adenoviral and transgenic expression of DKK-1, an inhibitor of the canonical Wnt signalling pathway, decimated the presence of mouse intestinal crypts.[6 7] Coupled to the predominance of canonical Wnt signals at the intestinal crypt-base, this led to the discovery that the Wnt target gene *lgr5* was enriched in mouse intestinal stem cells[8] and that ligation of this membrane receptor by the intestinotrophic factor R-spondin-1,[9] in conjunction with Wnt ligand-Fz-LRP5/6 complex formation,[10 11] synergistically activated Wnt signals. These seminal studies have given rise to the consensus that intense canonical Wnt signals at the crypt-base support intestinal stem cell biology (and Paneth cell differentiation in the small intestine) and that diminished Wnt signalling intensity along the crypt-axis is an important cue for progenitor proliferation, lineage specification, migration and shedding. Conversely, TGFβ/BMP signals predominate towards the open end of the crypt where they are thought to influence crypt cell positioning, differentiation and apoptosis.[12–15]

An analysis of gene expression patterns of normal human 'colon tops and basal crypts'[16] has detailed the topological expression of signalling pathway activators and inhibitors that are predicted to establish morphogenic gradients along the human colonic crypt-axis. Intriguingly, the respective activity of the Wnt signalling pathway at the crypt-base and the TGFβ/BMP pathway at the crypt-top is not thought not to be mutually exclusive. Reciprocal inhibition of the Wnt and TGFβ/BMP pathways appears to maintain the hierarchy and procession of tissue renewal along the crypt-axis. For example, genetic approaches in the mouse and analysis of human polyposis syndromes and colon cancer suggest that loss of TGFβ/ BMP pathway activation augments the Wnt signalling pathway, which disrupts tissue renewal and drives intestinal polyp/tumour formation.[12 14 15 17–19] In keeping with this notion, tissue culture conditions that favour Wnt pathway activation and inhibition of the TGFβ/BMP pathways have permitted the expansion ad infinitum of mouse and human intestinal organoids ex vivo. Strikingly, single crypts derived from the human colon spawn multiple budding structures[20] or expand into cyst-like spheroids,[21] each composed predominantly of immature stem/progenitor cells that can be induced to differentiate by withdrawal of Wnt stimulation, or used for therapeutic transplantation.[22] However, a detailed knowledge of the processes and signalling pathways involved in stem cell-driven tissue renewal in the human colonic epithelium is still lacking and is required to understand more fully the risk and pathogenesis of colorectal disease.

We have developed a culture model of near-native human colonic crypts that preserves crypt length, topology, morphology and cellular polarity.[23] Significantly, we now demonstrate that the hierarchy of stem cell-driven tissue renewal is recapitulated within this near-native human colonic crypt model ex vivo. Real-time imaging, gene reporter assays and dominant negative gene expression, in combination with subcellular immunolocalisation and in situ hybridisation, have been used to assess the status and mutual influence of Wnt and TGFβ/BMP signals on intestinal stem cell biology, proliferation, differentiation, migration and cell shedding in near-native human colonic crypts.

MATERIAL AND METHODS

Human colorectal tissue samples

This study was performed in accordance with approval from the East of England National Research Ethics Committee (LREC 97/124). Colorectal tissue samples were obtained with informed consent at rectosigmoid endoscopy from the sigmoid colon of 52 patients (51–83 years old) exhibiting no apparent intestinal pathology and from the normal mucosa (ie, >10 cm tumour margin) of 30 patients undergoing anterior resection (44–85 years old).

Microdissection of fixed native human colonic crypts

Biopsy tissue samples or surgical mucosal specimens were immediately fixed with 4% paraformaldehyde for 1 h and placed in phosphate-buffered saline. Single microdissected crypts were embedded in Matrigel, postfixed with 4% paraformaldehyde and processed for immunohistochemistry (see online supplementary methods).

Human colonic crypt isolation and culture

Colonic crypts were isolated as described previously,[23 24] embedded in Matrigel and placed into culture conditions that were similar to those described recently for intestinal organoids[20] and spheroids.[20 21] See online supplementary methods for details. BrdU (10 μM) was added to the experimental crypt culture media as described to monitor crypt cell proliferation and migration.

Adenoviral and lentiviral transduction

When required, freshly isolated colonic crypts were transduced with the lentiviral TOP-green fluorescence protein (GFP) Wnt reporter (HIV-based, VSV-G; SABiosciences) or adenoviral CMV-DN-TCF4 (type 5, dE1E3; Vector Biolabs) at a multiplicity of infection of 250 TU/crypt cell. Transduction with lentiviral or adenoviral CMV-GFP was used as a positive control to monitor infection efficiency.

Time-lapse videomicroscopy

Colonic crypts cultured in 12 well plates were placed on the climate-controlled (37°C, 5% CO_2) stage of a Nikon or Zeiss inverted motorised time-lapse system.

Whole mount immunohistochemistry and mRNA in situ hybridisation

Following embedding in Matrigel, microdissected-native crypts or cultured crypts were processed for immunohistochemistry or dual mRNA in situ hybridisation/immunohistochemistry. Immmunolabelling was visualised by using an appropriate combination of species-specific Alexafluor-conjugated secondary antibodies (Invitrogen). See online supplementary methods for details.

Reverse transcriptase polymerase chain reaction

Expression of marker genes for stem cells, differentiated crypt cell types and signalling pathway components was determined in freshly isolated and cultured crypts using quantitative or standard reverse transcriptase polymerase chain reaction (RT-PCR) techniques. See online supplementary methods for details.

Confocal microscopy

Following in situ hybridisation and/or immunohistochemistry, whole-mounted microdissected (ie, native) and cultured crypts were visualised by laser scanning confocal microscopy (Zeiss 510 META). A ×63 (1.4 numerical aperture) objective was used to obtain confocal images of the longitudinal crypt-axis. Image stacks were taken at 1–3 μm intervals which allowed selection of precise focal planes. The same acquisition parameters were used prior to post-hoc comparison of immunolabelling fluorescence intensity.

Image analysis

The crypt hierarchy was divided into three regions along the crypt-axis, each containing an equal number of nuclei and designated base, mid and top. In some cases, the base was subdivided into two regions of equivalent cell number, termed base and suprabase. The percentage number of cells (or nuclei) positive for a specific marker (eg, Ki67, LGR5), or the relative immunofluorescence intensity (eg, nuclear axin 2), was quantified (ImageJ, NIH) and expressed for each region; these values were either absolute or relative to the corresponding crypt-base value. Three dimensional images were rendered in Volocity (Improvision).

Statistical analysis

Data are expressed as means±SEM (n is the number of crypts derived from N patients). Differences between groups were determined using one-way analysis of variance (ANOVA) and Tukey's post-hoc method of multiple comparisons. Correlation between two variables was determined by the Spearman Rank test and independent association between variables was determined by the Chi Squared test. The level of significance (p value) is indicated in all cases.

RESULTS

Wnt, TGFβ and BMP signals correlate with the hierarchy of stem cell-driven tissue renewal in the human colonic epithelium

The hierarchy of tissue renewal in the native human colonic epithelium was characterised in crypts microdissected from colorectal biopsy tissue samples. Ki67 immunolabelling patterns depicted a prototypical profile of intense crypt cell proliferation in the lower half of the crypt-axis, including the presumptive stem cell zone at the crypt-base (figure 1A,B). Dual immunolocalisation and in situ hybridisation using high affinity oligonucleotide probes was used to visualise a population of slender LGR5-mRNA/OLFM4-positive cells (figure 1C,D; see online supplementary figure S1A) interspersed between MUC2-positive goblet-like cells (see online supplementary figure S1B) located at the base of native human colonic crypts. OLFM4 is a secretory protein[25] and was located at the mid-cell/juxtanuclear position and at the apical pole of the slender cytoplasm facing the crypt-lumen, where secreted OLFM4 protein was also present (figure 1C,D). *LGR5* mRNA labelling was perinuclear and some cells exhibited intense labelling in the mid-cell/juxtanuclear position (marked by arrowheads in figure 1C). Positive and negative controls for in situ hybridisation are shown in online supplementary figure S2. Immunolabelling using a monoclonal LGR5 antibody faithfully reproduced a similar pattern of labelling that was congruent with $OLFM4^+$ cells at the crypt-base (figure 1D). LGR5 protein was expressed on the basal membrane and within the cytoplasm of these slender crypt-base cells. As for *LGR5* mRNA in situ hybridisation, there was a subset of cells more intensely labelled with the LGR5 antibody (marked by arrowheads in figure 1D). Notably, the basal membranes of two $LGR5^+$ cells often wrapped around the basal membrane of an intervening goblet-like cell (see red arrowhead in figure 1D), which were negative for LGR5 and OLFM4 (see online supplementary figures S1B and S3B, respectively). Careful tracking in the z-dimension of E-cadherin-labelled single cell outlines, which often dipped in and out of any single confocal image plane, revealed a congruence of 96±4% for OLFM4 and either lgr5-mRNA or LGR5 protein expression; see online supplementary data for a schematic interpretation (see online supplementary figure S1A) and a 3D reconstruction (see online supplementary movie S1) of figure 1D. The $OLFM4^+/LGR5^+$ cell population predominates at the crypt-base (figure 1E) and at any one time, approximately half of the $OLFM4^+$ population is Ki67-positive (figure 1F), which is in keeping with the proliferative phenotype of mouse intestinal stem cells.[8]

An insight into the cellular signals that govern human intestinal tissue renewal was gained by spatially correlating signalling pathway activation along the hierarchy of the crypt-axis. Nuclear β-catenin, a hallmark of the canonical Wnt signalling pathway activation, and nuclear axin-2, a Wnt target gene, predominated at the crypt-base and exhibited an immunofluorescence intensity gradient that diminished along the crypt-axis (figure 2A,B). A high degree of congruence at the crypt-base was also exhibited by β-catenin and c-myc (another Wnt target gene) (see online supplementary figure S1D). Conversely, nuclear phospho-SMAD 2/3 immunofluorescence, an indicator of TGFβ pathway activation, peaked in the mid-crypt region (figure 2C), whereas nuclear phospho-SMAD 1/5/8 immunofluorescence, an indicator of BMP pathway activation, exhibited a retrogradient that was more intense at the crypt-opening (figure 2D). In accordance with similar observations made largely of the mouse intestine,[5–7 12 13 26] these findings suggested that active Wnt signals support human colonic crypt stem/progenitor cell proliferation and that TGFβ/BMP pathway activation may favour cell cycle withdrawal.

Combined activation of the Wnt pathway and inhibition of TGFβ/BMP pathways maintain native human colonic crypt morphology in culture

In order to investigate the functional influence of Wnt and TGFβ/BMP signalling pathways on renewal of the human colonic epithelium, we refined a native human colonic crypt culture model.[23] Following on from the signalling pathway profiles described in figure 2 and the conditions developed for intestinal organoid propagation,[20 21 27] optimisation of human colonic crypt culture conditions was based on generating Wnt

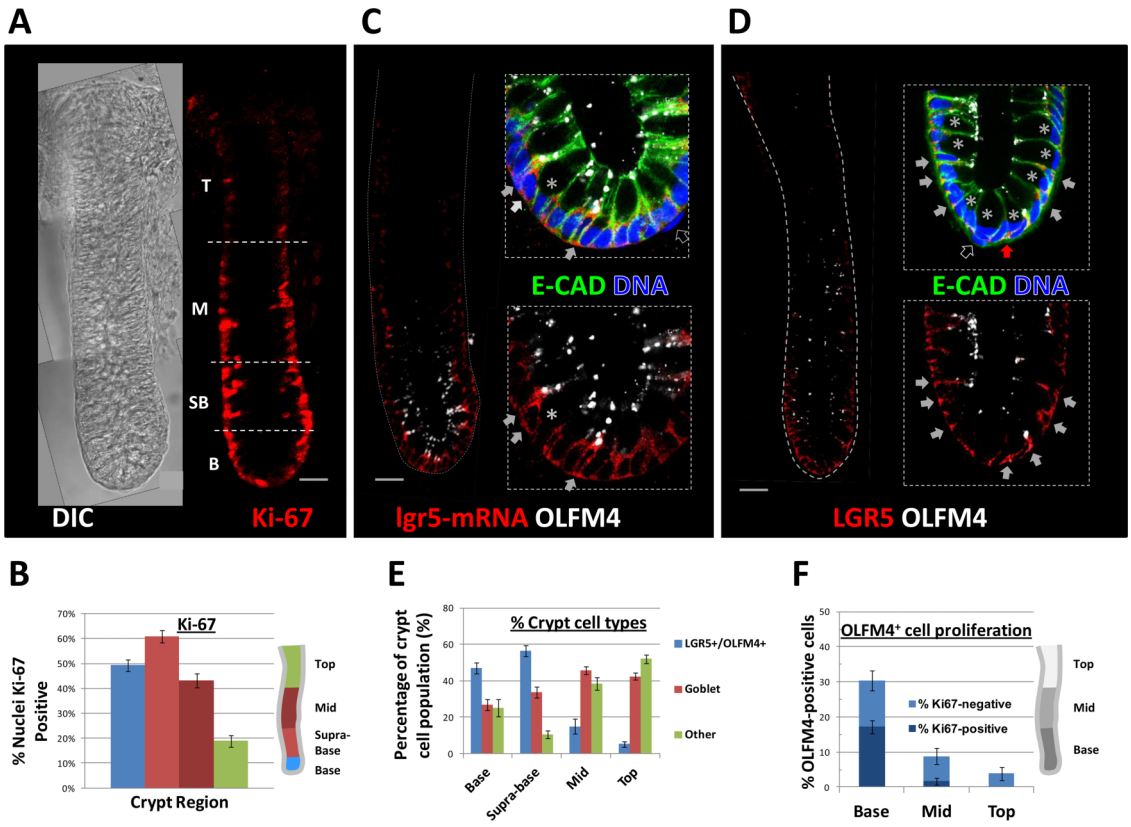

Figure 1 Hierarchy of stem/progenitor cell proliferation along the native human colonic crypt-axis. (A) Classical profile for Ki-67 immunolabelling (red) of microdissected (ie, native) human colonic crypts; B-base, SB supra-base, M-mid, T-top. (B) Ki67-positive cell nuclei predominate at the crypt-base and the mid-crypt region (N=13 subjects, n=58 crypts). (C) Dual in situ hybridisation and immunolabelling of lgr5-mRNA (red) and OLFM4 protein (white) identifies a population of lgr5-mRNA+/OLFM4+cells at the base of native human colonic crypts; E-CAD (green) demarks crypt cell membranes; filled white arrows indicate cells exhibiting intense fluorescent labelling for lgr5-mRNA and OLFM4; open arrow denotes nucleus of pericryptal myofibroblast; asterisk signifies a goblet cell with nucleus in the confocal image plane; scale bar—30 mm. (D) Double immunolabelling of LGR5 protein (red) and OLFM4 (white) confirms congruent expression of both intestinal stem cell markers by individual crypt cells within the crypt-base; annotations as above; see online supplementary figure S1 for schematic representation. (E) Quantification of cell types according to stem cell marker expression and cell morphology along the crypt-axis (see online supplementary figure S1 for an example, of lgr5-mRNA/MUC-2 double labelling); the congruence of OLFM4 and either lgr5-mRNA or LGR5 protein expression was 96%±4% (mean±SD, n=20 microdissected crypts from N=4 subjects). (F) Analysis of crypt stem/progenitor cell proliferation (n=10 crypts from N=5 subjects; see online supplementary figure S1 for a crypt image of double OLFM4/Ki-67 immunolabelling). Arrows indicate examples of intense labelling for lgr5+/OLFM4+ stem cells. *Denotes an example of a goblet cell with nucleus in plane of focus. DIC, differential interference contrast; E-CAD, E-cadherin.

signals and suppressing TGFβ/BMP signals ex vivo. A range of growth factors in various combinations were tested with the aim, in the first instance, of maintaining near-native crypt length, topology, morphology and polarity (figure 3A,B, see online supplementary figure S4). Significantly, canonical Wnt pathway activation by Wnt-3A and/or R-Spondin-1 was insufficient to maintain human colonic crypt length (figure 3D) or viability beyond 4 days (not shown). However, in combination with the BMP antagonist Gremlin-1[16] or noggin,[8] the intestinotrophic factor IGF-1,[28] and an ALK4/5/7 inhibitor A83–01 (or SB431542, not shown), crypts maintained their length and morphology for at least 7 days in culture (figure 3C,D) when the Matrigel became unstable. These conditions were conducive for crypt cell proliferation and migration as observed under digital video time-lapse microscopy (see online supplementary movies S2 and S3). Conversely, colonic crypt length and morphology were compromised by inhibition of canonical Wnt signals or by imposing either TGFβ or BMP signals (see online supplementary figure S5). Of note, replacing IGF-1 with EGF promoted remodelling of human colonic crypt morphology followed by multiple budding events characteristic of intestinal organoid growth (see online supplementary figure S6).[20]

Colonic crypt Wnt signals are inhibited by TGFβ or BMP pathway activation

To determine activation of the canonical Wnt signalling pathway, human colonic crypts were treated with Wnt-3A in the presence or absence of DKK-1. Wnt-3A stimulated translocation of nuclear de-phospho-β-catenin and this was inhibited by DKK-1 (figure 4A). Wnt-3A treatment also induced nuclear accumulation of the Wnt target gene Axin-2, which was inhibited by transduction of crypts with an adenoviral vector carrying a dominant negative TCF4 mutant (figure 4B). Exogenous Wnt-3A also stimulated TOP-GFP intensity confirming activation of Wnt target gene transcription (figure 4C). Treatment of crypts with an inhibitor of Wnt production, IWP2 (2 μM), suppressed basal TOP-GFP expression (figure 4C) and basal levels of nuclear axin-2 (figure 4D), both of which were rescued by addition of exogenous Wnt-3A. Wnt-3A mRNA was found to be expressed in freshly isolated crypts by RT-PCR and Wnt-3A ligand was immunolocalised to the stem cell region at the human colonic crypt-base (figure 4E).

TGFβ and BMP signalling pathway status in cultured human colonic crypts was assessed by phospho-SMAD immunofluorescence. A83–01 suppressed the TGFβ-induced increase in nuclear

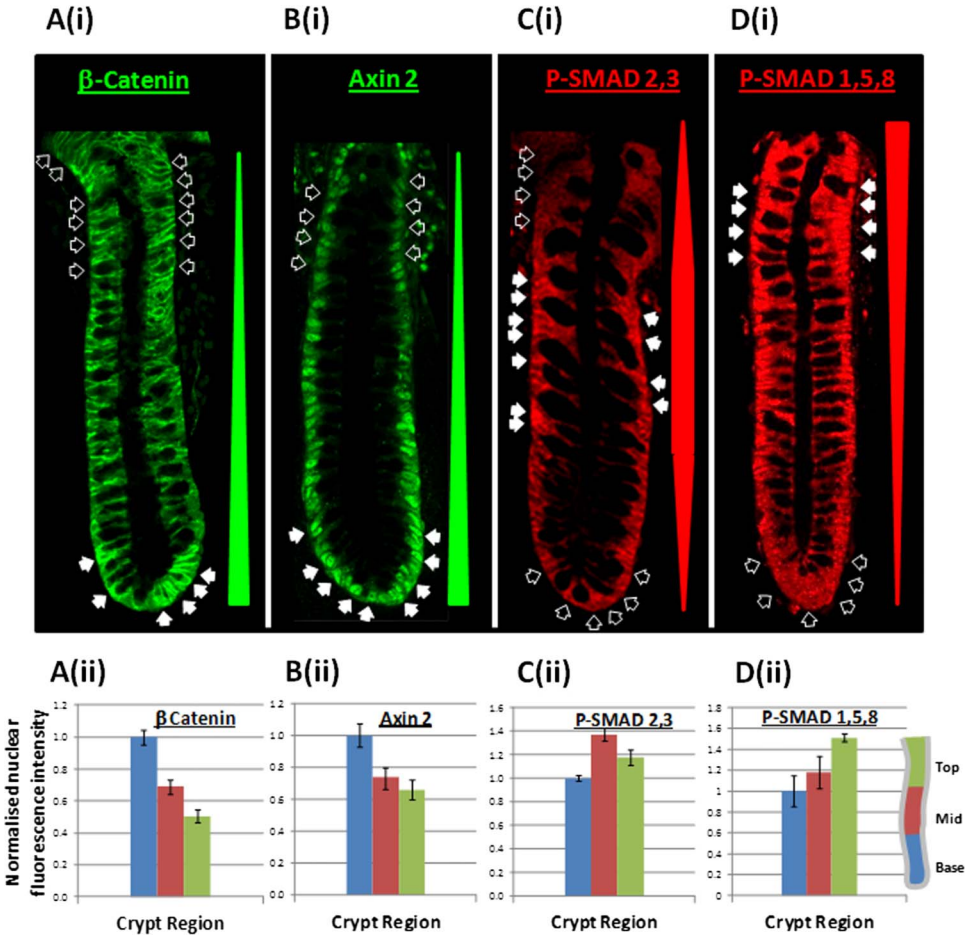

Figure 2 Wnt/β catenin and SMAD signalling profiles along the native human colonic crypt-axis. (Ai) Immunolabelling of total β catenin performed on native human colonic crypts reveals intense membrane and nuclear localisation at the colonic crypt-base. (Aii) The fluorescence intensity of nuclear β catenin predominates at the crypt-base and diminishes progressively towards the top of the crypt (Spearman Rank, r=−0.47, p<0.001). (B) A similar gradient exists for the immunofluorescence intensity of nuclear Axin-2 labelling (r=−0.48, p<0.001). Conversely, the immunofluorescence for nuclear phospho-SMAD 2,3 (C) predominates in the mid-crypt region, while nuclear phospho-SMAD 1,5,8 (D) exhibits a retrogradient that is more intense at the crypt opening (r=0.84, p<0.04). All values in each bar chart were normalised to the intensity value at the crypt-base. For each antibody, data were collated from n≥10 crypts microdissected from N≥3 patients. Filled arrowheads indicate intense nuclear labelling; open arrowheads mark nuclei of lower fluorescence intensity.

phospho-SMAD 2,3 levels (figure 5A), while noggin inhibited BMP stimulation of nuclear phospho-SMAD 1,5,8 levels (figure 5B). TGFβ and BMP inhibited the levels of nuclear axin-2, which was rescued by A83-01 (figure 5C) and noggin (figure 5D), respectively. It is noteworthy that A83-01 and noggin also augmented nuclear axin-2 levels in the absence of exogenous TGFβ or BMP ligand (figure 5C,D). These studies demonstrate that the Wnt signalling pathway in human colonic crypts is suppressed by TGFβ or BMP pathway activation. However, under optimal culture conditions, that is, Wnt stimulation in conjunction with BMP/ TGFβ suppression, the axin-2, p-SMAD 2,3 and p-SMAD 1,5,8 signalling gradients observed along the native human colonic crypt-axis (figure 2) were maintained ex vivo (see online supplementary figure S7). Also, analysis of marker genes for stem cells and differentiated crypt cell types indicated that the relative levels of gene expression in native crypts were similar to those placed in culture (see online supplementary figure S8). Taken together, these observations provided a good basis on which to investigate the relative influence of Wnt, BMP and TGFβ signalling pathways on human colonic crypt cell renewal.

Canonical Wnt signals support, and TGFβ/BMP signals inhibit, human colonic crypt stem/progenitor cell proliferation

Inspection of bright-field time-lapse movies (see online supplementary movies S2 and S3) revealed regular movements of cell nuclei and membranes in the proliferative zone of the crypt that were evocative of crypt cell mitoses. Accordingly, Wnt signals stimulated BrdU uptake and Ki67 labelling of cells located in the lower-half of human colonic crypts ex vivo (figure 6A,B). Inhibitors of Wnt signal transduction (DKK-1) and Wnt target gene activation (DN-TCF4 expression) abrogated Wnt-stimulation of human colonic crypt cell proliferation (figure 6A, B). Significantly, a population of LGR5$^+$/OLFM4$^+$ slender cells were interspersed between goblet-like cells within the cultured colonic crypt-base (figure 6C) in similar numbers found in the native crypt (*cf.* figures 1E and 6D,E). OLFM4 expression was inhibited by DKK-1 (figure 6D), as was *LGR5*-mRNA (not shown). An inhibitor of Wnt ligand secretion, IWP2, suppressed basal levels of LGR5 immunofluorescence and this was rescued by exogenous Wnt-3A (figure 6E,F); exogenous Wnt-3A also increased stem cell proliferation along the crypt-axis (figure 6G).

Human colonic crypts cultured over a period of at least 1 week continued to express markers of goblet (MUC-2), tuft (COX-1), enterocyte (FABP1) and enteroendocrine (chromogranin A) cell types (figure 6H) with a similar labelling pattern to that observed in native colonic crypts (see online supplementary figure S3). The ability of stem/progenitor cells to differentiate in culture was investigated by treating crypts with the notch inhibitor dibenzazepine. Crypt cells exhibited an increased number of MUC2$^+$ goblet cells (figure 6H,I)[20 21] and a decreased number of OLFM4$^+$ cells (figure 6J).[29]

The observations described thus far demonstrate that Wnt signals are prominent at the base of human colonic crypts and support intestinal stem cell biology and crypt cell proliferation. Given that TGFβ and BMP signals suppress Wnt signals (figure 5), it followed that they would also inhibit crypt cell proliferation. Accordingly, BrdU uptake was suppressed by omission of the BMP inhibitor noggin or the TGFβ inhibitor A83-01 (figure 7A,C). Exogenous BMP or TGFβ abolished BrdU uptake, which was rescued by noggin or A83-01, respectively (figure 7A,C). A

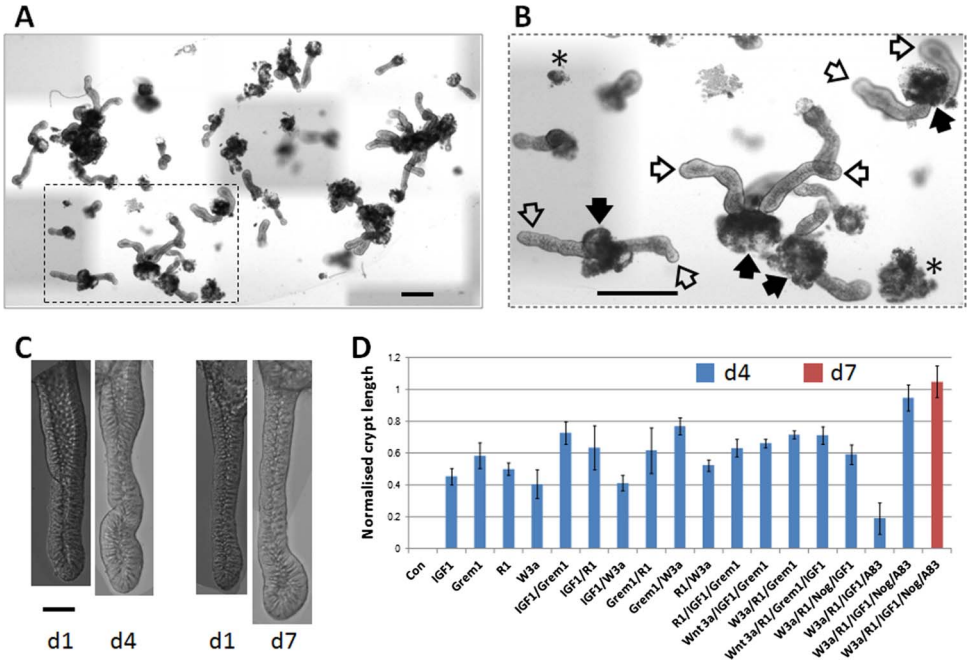

Figure 3 A combination of Wnt pathway activators and TGFβ/BMP pathway inhibitors is required for maintenance of cultured human colonic crypts ex vivo (A) Overview of human colonic crypts cultured within a Matrigel droplet under optimised conditions described in panel D; the bright field image was created by stitching together an array of 12 adjacent fields of view taken with a ×4 objective lens; scale bar=0.5 mm. (B) Enlargement of insert depicted in (A) representing a typical field of view (×4 objective lens); example crypt-base and shedding domains are denoted by open and closed arrowheads, respectively; *dead crypt fragments; scale bar=0.5 mm. (C) Example paired differential interference contrast images (×20 objective) of human colonic crypts cultured under optimised conditions for 0–4 and 0–7 days; d1=day 1, d4=day 4, d7=day 7; scale bar=100 μm. (D) Quantification of crypt length at day 4 or day 7 (with respect to the initial crypt length 4 h post-isolation, Day 0) following culture in the presence of the indicated combination of recombinant human growth factors, recombinant human BMP binding protein and/or small molecule ALK 4/5/7 inhibitor: IGF-1 (50 ng/mL), Gremlin-1 (200 ng/mL), Noggin (100 ng/mL), Wnt3A (100 ng/mL), R-Spondin-1 (500 ng/mL), A83-01 (0.5 μM); n≥6 crypts derived from N≥3 subjects.

neutralising pan-specific TGFβ antibody mimicked the effects of A83-01 (figure 7B) and a specific small molecule inhibitor of BMPR2/ALK2, DMH-1, reproduced the effect of noggin (figure 7D). In addition, activation of the BMP or TGFβ pathway abolished LGR5 expression (figure 7E).

Canonical Wnt signals combined with suppressed TGFβ/BMP pathways are permissive for tissue renewal ex vivo

The relative upward movement of crypt cells along the crypt-axis from the crypt-base was demonstrated by a classical BrdU pulse-chase approach (figure 8A). Inhibition of Wnt signalling with DKK-1 blocked the upward movement of BrdU pulse-labelled cells in the lower half of the crypt-axis into the upper-half of the crypt-axis (figure 8B). In addition to this relative migration of cells within the crypt frame of reference, absolute cell migration was also observed when crypts were cultured under suboptimal culture conditions (ie, reduced Wnt stimulation). Absolute crypt cell migration was associated with shortening of the crypt length (eg, see online supplementary figure S5), whereby the crypt-base migrated towards the crypt opening and crypt cells were shed from the surface (figure 8D). To explore the link between crypt cell proliferation and migration, crypts were cultured under conditions that imposed different levels of proliferation and were observed under time-lapse microscopy. Crypt length (figure 8Ci) and crypt cell proliferation followed a similar decreasing trend under culture conditions endowed with less proliferative potential (*cf.* figure 8Ci,Cii), but crypt cell migration rate stayed constant (figure 8Ciii). The average migration rate for crypts exhibiting a steady state length was 4.95±0.45 μm/h (n=20 crypts, N=4 patients). Cell shedding was localised to the upper crypt region as revealed by labelling of 'live' cultured crypts incubated with live/dead fluorophores, that is, calcein/propidium iodide (figure 8Di) and by immunolabelling fixed crypts for activated-caspase-3 (figure 8Dii). The accumulation of shed cells at the crypt opening was monitored in real time by observing discrete, intense bursts of red fluorescence associated with propidium iodide binding to cell nuclei following membrane rupture (figure 8Ciii and online supplementary movie S4). Thus, under these conditions, crypt cell proliferation in the lower half of the crypt is required to maintain a steady-state crypt cell population (eg, constant crypt length) by replenishing cells shed from the upper surface, but does not appear to drive (ie, mitotic pressure) crypt cell migration per se.

DISCUSSION

Intestinal tissue renewal is fundamental to long life and lifelong health. The processes by which the intestinal epithelium renews itself have been well described in the mouse, but the molecular and cellular mechanisms that govern tissue renewal in the human gut are less well understood. Central to gaining a more detailed understanding is the development of model systems for the native human intestinal epithelium. Ideally, these should recapitulate the processes of tissue renewal in health and disease. Another desirable requirement is that ex vivo human tissue models are amenable to bioimaging and functional genomic approaches. Complementary to the recent development of intestinal organoid culture systems, we have developed a culture model of near-native human colonic crypts. Presently, we have demonstrated a requirement for canonical Wnt signals and suppressed TGFβ/BMP pathways to support intestinal stem

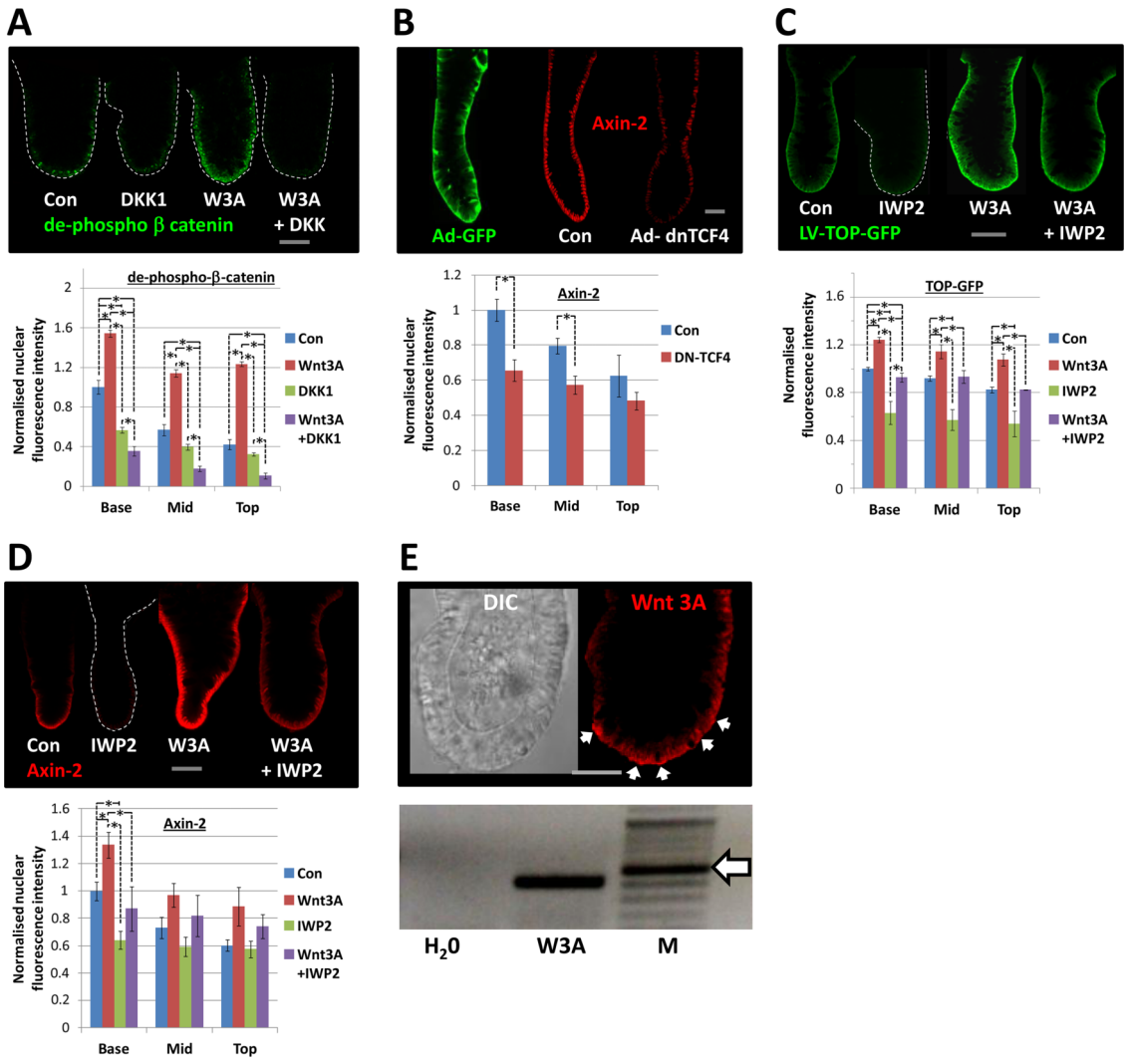

Figure 4 Exogenous and crypt-autonomous Wnt ligand promotes canonical Wnt/β catenin signals in cultured human colonic crypts. (A) Confocal images of dephospho β catenin immunolabelling following treatment with exogenous Wnt-3A (100 ng/mL, 30 min), in the presence or absence of Dikkopf-1 (DKK-1; 800 ng/mL); bar chart illustrates image analysis of nuclear immunofluorescence intensity. (B) Visualisation and analysis of nuclear Axin-2 3 days post-transduction with adenoviral GFP (Control: green Ad-GFP; red—Axin2) or dominant negative-TCF4. Effects of IWP2 (2 μM) on lentiviral (LV)-TOP-GFP expression (C) and nuclear axin-2 (D) immunofluorescence following 3 days culture. (E) Immunolabelling of human Wnt-3A (arrows indicate intense labelling basal membranes) and expression of Wnt-3A mRNA by RT-PCR using cDNA from freshly isolated human colonic crypts; expected Wnt 3A PCR product is 404 bp and the arrow denotes a 500 bp marker. All values in (A)–(D) bar charts were normalised to the control value in the crypt-base region. Control media: for A, C and D=IGF-1 (50 ng/mL)/Noggin (100 ng/mL)/R-spondin-1 (500 ng/mL); Wnt-3A (100 ng/mL) where indicated; for B=IGF-1 (50 ng/mL)/Noggin (100 ng/mL)/R-spondin-1 (500 ng/mL)/Wnt-3A (100 ng/mL). Statistical significance assessed by ANOVA followed by Tukey's post-hoc analysis; significant differences between pairs of mean values are indicated by linked dashed lines, *p<0.01; n≥4 crypts for each experimental group and the data are representative of at least three independent experiments in each case.

cell-driven tissue renewal in the human colon. Non-repressed TGFβ/BMP signals inhibited the canonical Wnt signalling pathway, intestinal stem cell marker expression and crypt cell proliferation, while unabated crypt cell migration and shedding resulted in the appearance of drastically shortened crypts and a compromised crypt cell population.

Intestinal stem cells play a central role in tissue renewal and a strategy to label these cells in situ was imperative. Lineage tracing,[8] propagation of self-renewing intestinal organoids[27] and transplantation[22] assays have defined LGR5 as a marker of proliferative intestinal stem cells. Characterisation of the mouse small intestinal stem cell transcriptome identified a number of highly enriched genes including OLFM4,[30] which, although not expressed in the mouse colon, was also enriched in human colonic stem cells.[21 31] The current study used confocal imaging of whole-mounted intact human colonic crypts to visualise double labelling of OLFM4 protein and either LGR5 protein or LGR5-mRNA at subcellular resolution. We identified a number of $LGR5^{+}$/$OLFM4^{+}$ slender cells at the base of human colonic crypts, interspersed between goblet-like cells. This is reminiscent of the case for LGR5-GFP positive cells in the mouse colon.[32] A subpopulation of $LGR5^{+}$/$OLFM4^{+}$ cells existed that were more intensely labelled with LGR5 protein or mRNA (figure 1C,D). By analogy with sorting of single $LGR5^{GFP\text{-}Hi}$ cells from the mouse intestine[32] and $EPHB2^{Hi}$ (a surrogate marker for LGR5-positive cells) cells from the human colon,[21] it is likely that immunolabelling of $LGR5^{Hi}$/$OLFM4^{+}$ cells indicate the human intestinal stem cells proper and that $LGR5^{Lo}$/$OLFM4^{+}$ are progenitors. Indeed, OLFM4 mRNA expression has been shown to extend beyond $LGF5^{Hi}$ cells.[26 33] It is also noteworthy that recent observations of the mouse intestine

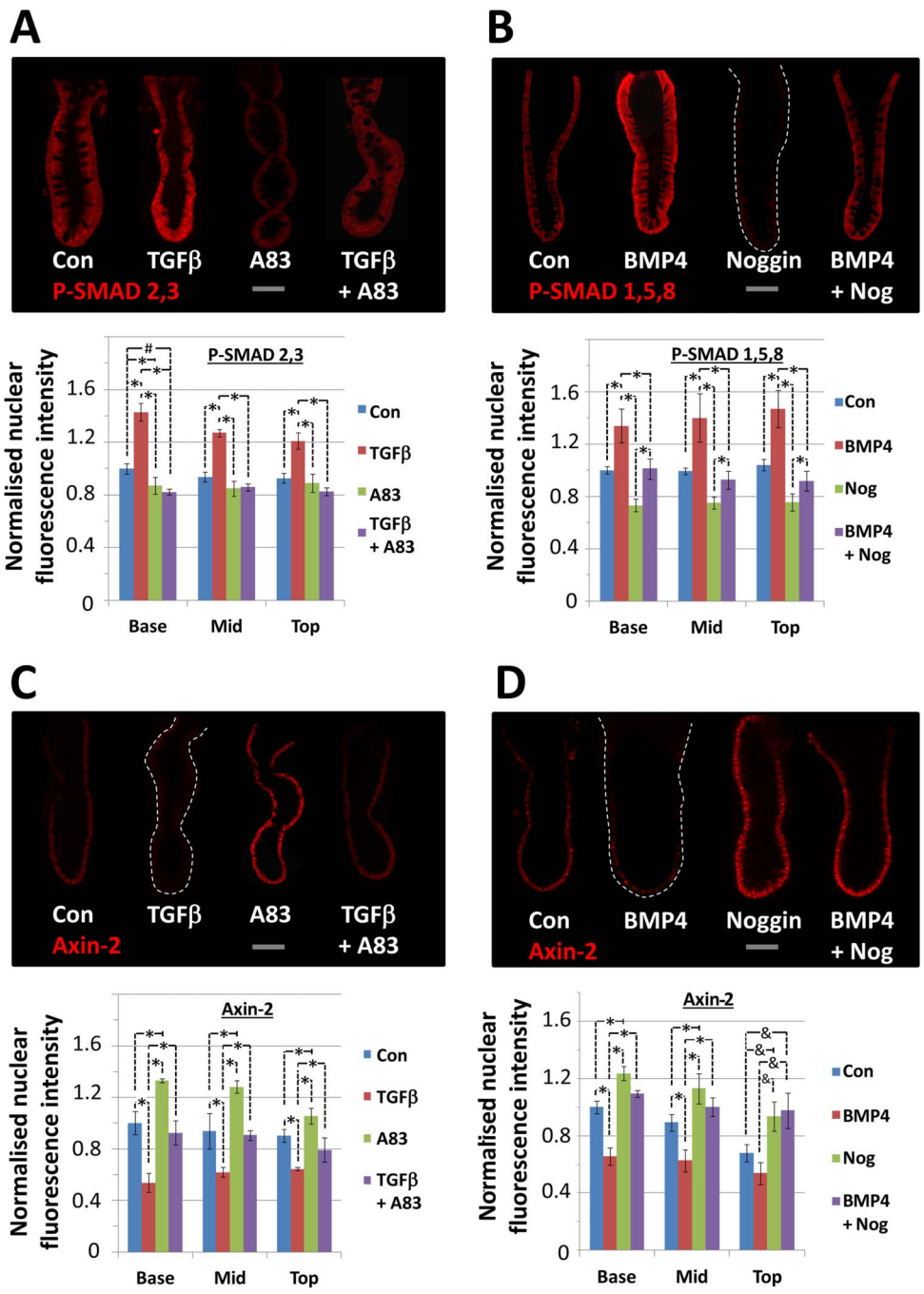

Figure 5 TGFβ and BMP pathway activation inhibits canonical Wnt signalling along the cultured human colonic crypt-axis. (A) Confocal images of phospho-SMAD2,3 immunolabelling following treatment with TGFβ (20 ng/mL, 2 days), in the presence or absence of A83-01 (0.5 μM); bar chart illustrates image analysis of nuclear immunofluorescence intensity. (B) Effects of BMP (100 ng/mL, 2 days) and/or noggin (100 ng/mL) on nuclear phospho-SMAD1,5,8 immunofluorescence intensity levels. (C) TGFβ and (D) BMP suppression of nuclear Axin-2 immunofluorescence, and rescue by pretreatment with noggin or A83-01, respectively. All values in (A–D) were normalised to the control value in the crypt-base region. Culture conditions: (A and C)—IGF-1 (50 ng/mL)/R-spondin-1 (500 ng/mL)/Wnt-3A (100 ng/mL)/Noggin(100 ng/mL) and TGFβ (20 ng/mL) and/or A83-01 (0.5 μM) where indicated; (B and D)—IGF-1 (50 ng/mL)/R-spondin-1 (500 ng/mL)/Wnt 3A (100 ng/mL)/A83-01 (0.5 μM) and BMP (100 ng/mL) and/or noggin (100 ng/mL) where indicated. Significant differences were assessed by ANOVA followed by Tukey's post-hoc analysis; significant differences between pairs of mean values are indicated by linked dashed lines; $^{\#}p<0.01$, $^{*}p<0.02$, $^{\&}p<0.05$; n≥4 crypts for each experimental group and the data are representative of at least three independent experiments in each case. Scale bars=75 μm.

point to increased plasticity of crypt progenitor cells in that they can dedifferentiate into intestinal stem cells following injury.[34] In this respect, it will be fascinating to determine the precise relationship between $LGR5^{Hi}$/$OLFM4^{+}$ cells, $LGR5^{Lo}$/$OLFM4^{+}$ cells and stem cell potential following injury, and with respect to ageing and cancer risk.[35]

A functional role for morphogen gradients in conferring a crypt stem/progenitor phenotype was indicated by distinct profiles of signal pathway activation along the crypt-axis (figure 2). Substituting EGF with IGF-1 restrained the formation of multiple buds that is associated with mass expansion of intestinal stem cells in organoid culture.[20 21] These modified conditions

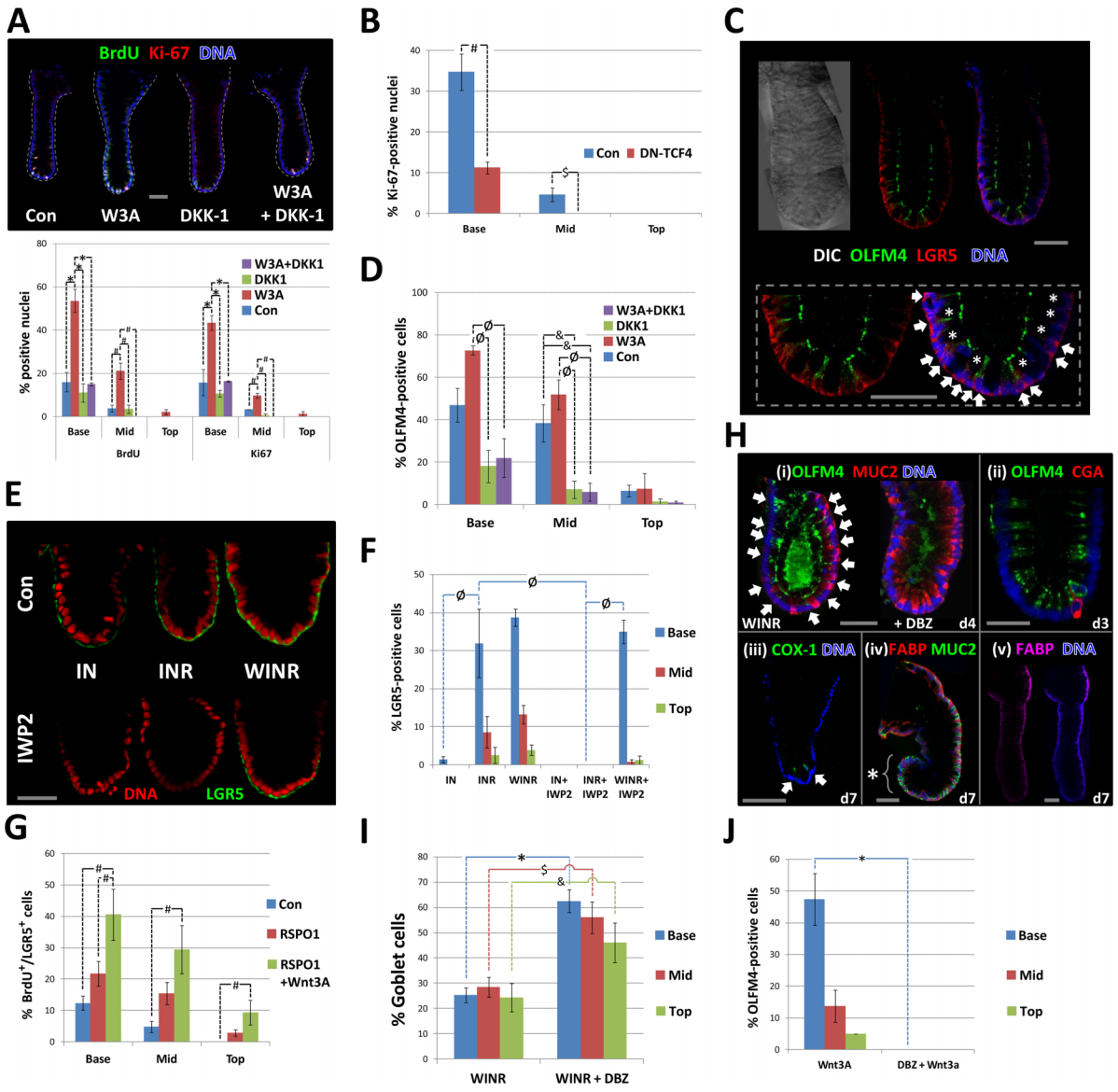

Figure 6 Canonical Wnt signals maintain cultured human colonic crypt stem/progenitor cell proliferation. (A) Effects of exogenous Wnt-3A (100 ng/mL) and/or DKK-1 (800 ng/mL) on nuclear BrdU uptake and Ki67 labelling after 3 days culture. (B) Dominant-negative TCF4 abrogates crypt cell proliferation 3 days post-transduction. (C) Coexpression of OLFM4 and LGR5 by a population of slender cells (arrowheads) interspersed between goblet-like cells (asterisk) located at the base of human colonic crypts cultured for 4 days. (D) The relative effects of Wnt-3A (100 ng/mL) and DKK-1 (800 ng/mL) on the percentage of OLFM4-positive cells following 3 days in culture. (E) Confocal images and (F) image analysis of LGR5 immunolabelling following 4 days in culture: suppression by IWP2 (2 μM) and rescue by exogeneous Wnt-3A (100 ng/mL). (G) Wnt pathway activators promote BrdU incorporation into the nuclei of LGR5-positive colonic crypt cells. (H) Immunolabelling of differentiated cell types in cultured colonic crypts: distinct labelling of cells positive for (i) MUC-2 or OLFM4 (arrows), (ii) chromogrannin A or OLFM4, and (iii) COX-1; all shown at the base of human colonic crypts; (iv, v) intense FABP1 labelling at the crypt opening (asterisk and bracket indicate crypt-base). The effects of the Notch inhibitor, DBZ (1 mM) on goblet cell number and OLFM4-positive cell number illustrated in (H) are quantified in (I and J), respectively. Significant differences were assessed by ANOVA followed by Tukey's post-hoc analysis; significant differences between pairs of mean values are indicated by linked dashed lines; *$p<0.001$, $^{\$}p<0.002$, $^{\varnothing}p<0.02$, $^{\#}p<0.01$, $^{\&}p<0.05$. Scale bars=50 μm. Control media: I=IGF-1 (50 ng/mL), N=Noggin (100 ng/mL), R=R-spondin-1 (500 ng/mL), A83-01 (0.5 μM); W3A or W=Wnt-3A (100 ng/mL), DKK-1 (Dikkopf-1; 800 ng/mL) and DBZ=dibenzazepine (1 mM) where indicated.

supported the homeostatic renewal of the crypt cell population by maintaining the hierarchy of crypt cell proliferation, migration, differentiation and shedding, while the crypt length remained relatively constant. Cultured crypts exhibited a similar $OLFM4^+/LGR5^+$ cell number and proliferative activity to that observed for native crypts. Mitotic events in human colonic crypts were very distinctive: a nucleus migrated from the basal pole to the apical pole of the cell, while the cell membrane apparently maintained contact with the basement membrane via a pedestal; following cytokinesis, the daughter nuclei returned to the apical pole (see online supplementary movies S2 and S3). All barring a few of the observed mitotic events (>1000) occurred at the apical pole with only a few noticeable events at the basal pole. A comprehensive analysis of spindle orientation is yet to be conducted. The observed crypt cell migration rate of ~5 μm/h predicts a renewal cycle of just over 3 days for a crypt of length 400 μm. Significantly, crypt cell migration continued in the relative absence of crypt cell proliferation, as has been

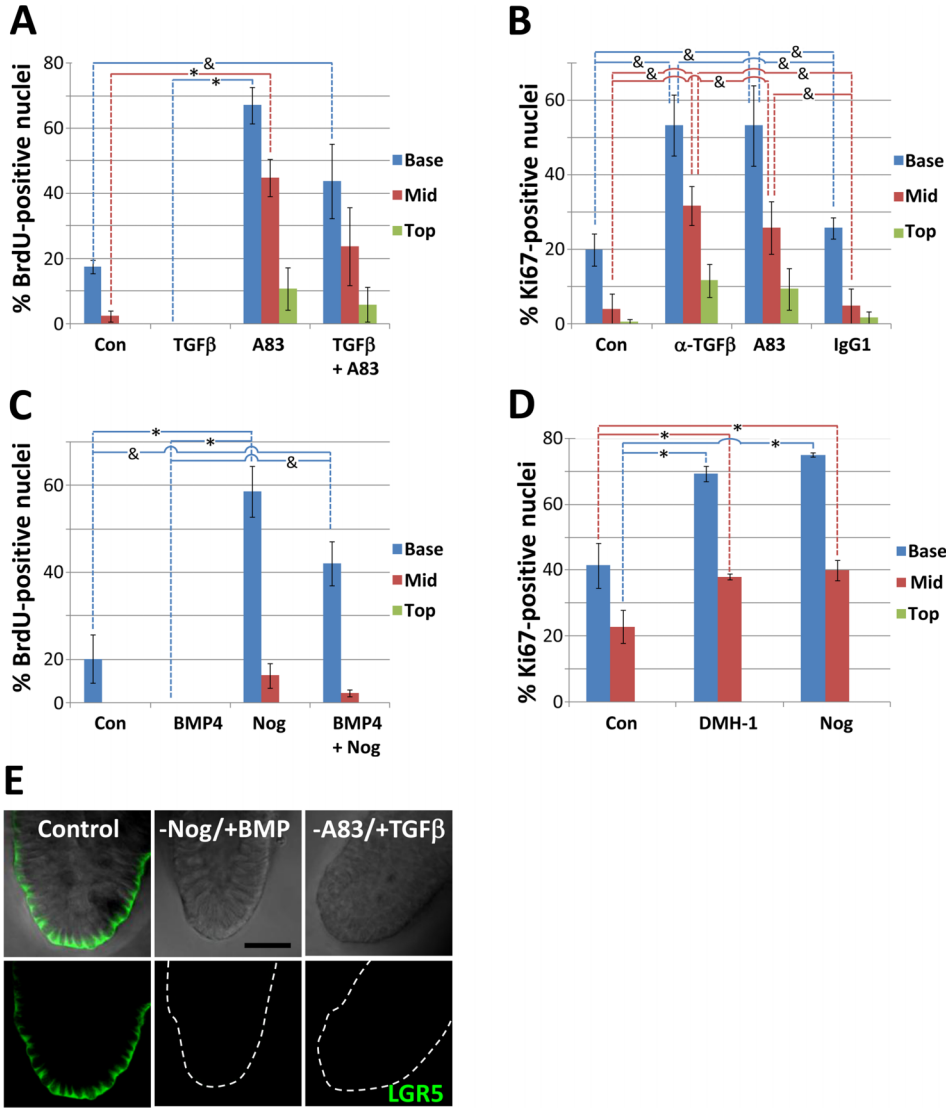

Figure 7 Activation of TGFβ or BMP pathways suppress cultured human colonic crypt stem/progenitor cell proliferation. (A) Effects of treatment with TGFβ (20 ng/mL, 2 days) and/or the ALK4/5/7 inhibitior A83-01 (0.5 μM) on nuclear incorporation of BrdU incorporation into human colonic crypt cells. (B) A pan-specific monoclonal TGFβ antibody (10 μg/mL) mimicks the effects of A83-01 (0.5 μM) on crypt cell proliferation; the irrelevant monoclonal anti-COX2 (10 μg/mL) was included as an IgG1 control. (C) BMP (100 ng/mL) abolishes human colonic crypt cell proliferation. Noggin (100 ng/mL) promotes crypt cell proliferation and prevents the inhibitory effects of BMP4. (D) The BMPR1 (ALK2/3) inhibitor DMH-1 (1 μM) mimics the stimulatory effects of noggin on crypt cell proliferation. (E) BMP pathway or TGFβ pathway activation suppress LGR5 immunolabelling. Significant differences were assessed by ANOVA followed by Tukey's post-hoc analysis; significant differences between pairs of mean values are indicated by linked dashed lines; *p<0.001, &p<0.05; n≥4 crypts for each experimental group and the data are representative of at least three independent experiments in each case. Control media: (A and B) W/I/N/R; (C and D) W/I/R/A83-01; (E) W/I/N/R/A83-01. W=Wnt 3A, I=IGF-1, 'N' or 'Nog'=noggin, R=R-spondin-1.

reported for the mouse intestine in vivo.[36] Cell shedding occurred in an organised manner and cells did not lose membrane integrity until they were extruded from the cell monolayer. Although known to stimulate colon cancer cell lines, the actions of IGF-1 on the native human colonic epithelium are not that well described.[28] IGF-1 stimulated crypt cell proliferation (not shown) and it will be informative to investigate the potential for Wnt signalling pathway transactivation.[37]

Exogenous Wnt ligand was required for human colonic crypt culture. Maintenance of a Wnt signalling gradient sustained the hierarchy of tissue renewal for at least 7 days. However, in the first few days of culture in the absence of exogenous Wnt ligand, crypts exhibited basal levels of Wnt signal activation, stem cell marker expression and cell proliferation. These traits were abolished by IWP2, an inhibitor of Wnt ligand secretion.[38] In support of crypt cell-autonomous secretion of Wnt ligand, isolated crypts expressed *Wnt 3A* mRNA and immunolabelling for Wnt 3A identified positive cells within the stem cell niche at the crypt-base. However, in contrast to mouse Paneth cells (a source of Wnt ligand for neighbouring small intestinal stem cells) mouse colonic crypts do not express Wnt ligand and would appear to be completely reliant on Wnt stimulation from subepithelial sources.[39] The present observations in human colonic crypts point to a key role for the colonic crypt Wnt signalling gradient in regulating intestinal stem cell status and tissue renewal. Wnt signalling status varies along the longitudinal gut-axis[40] and is thought to be subject to epigenetic modulation in relation to ageing and cancer.[41 42] Disruption of the colonic crypt Wnt signalling gradient would be expected to impact on crypt renewal homeostasis and influence disease risk. In fact, higher concentrations of Wnt 3A ligand caused mass expansion of intestinal stem/progenitor cells along the crypt-axis (not shown) and we are currently investigating the consequences to crypt cell renewal and the relevance to disease onset.

The colonic crypt signalling Wnt gradient is subject to influence by other morphogens. Cross-talk between Wnt and TGFβ/BMP pathways has been documented in the mouse intestine in vivo[14 15 43] and ex vivo[44] via transcriptional[15] and non-transcriptional[14] regulation of β catenin. Here we demonstrate that TGFβ/BMP downregulates Wnt signals in human colonic crypts and suppresses stem cell marker and stem/progenitor cell proliferation as a consequence. In a more spatially defined context, it has been demonstrated in the mouse that de novo crypt regeneration following injury is dependent on the confined induction of TGFβ expression. The resulting localised inhibition of crypt cell proliferation, in combination with maintained Wnt signalling in the vicinity, throws the epithelium into nascent crypt domains.[26]

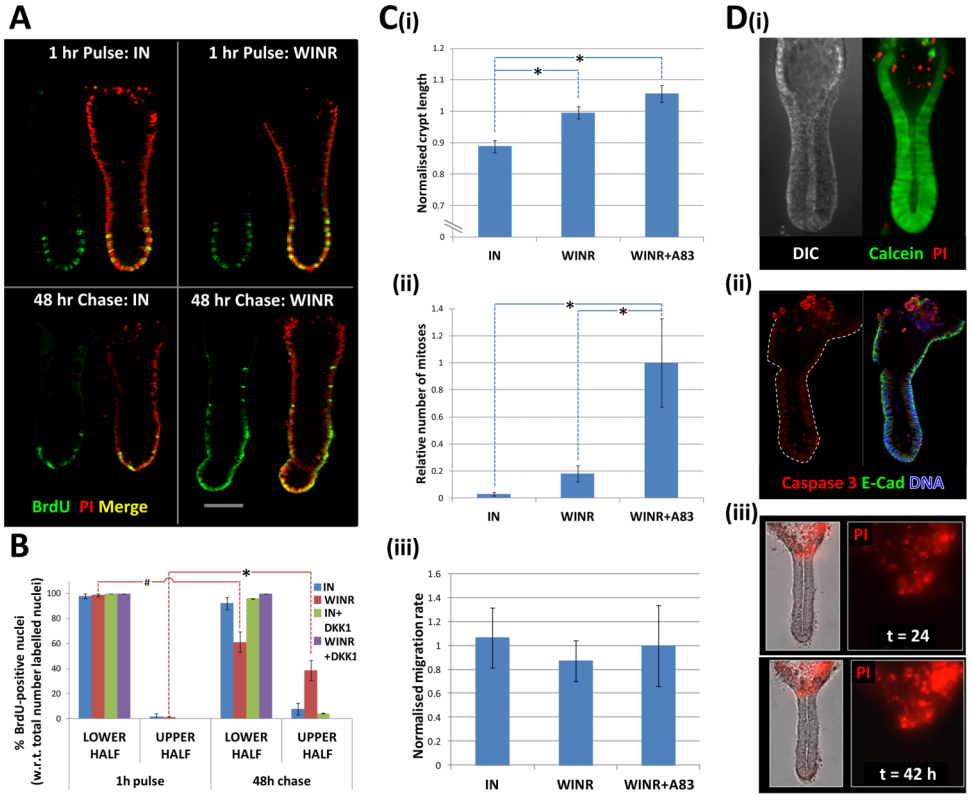

Figure 8 Crypt cell migration and shedding complete tissue renewal ex vivo. (A) A BrdU pulse-chase experiment demonstrating the relative upward migration of cells from the crypt-base along the crypt-axis in the absence (IGF-1, 50 ng/mL and Noggin, 100 ng/mL) or presence of Wnt stimulation (Wnt-3A, 100 ng/mL and R-spondin-1, 500 ng/mL); for each condition, images are shown 1 h following the BrdU pulse and 2 days after the 'cold' chase. (B) Analysis of BrdU pulse-chase images illustrating the respective decrease and increase in BrdU-positive crypt cells in the lower and upper half of the crypt in the presence of Wnt stimulation. (C) Analysis of time-lapse data acquired during days 2–3 in culture under different degrees of Wnt and TGFβ signalling pathway activation; relative changes in crypt length (Ci) and crypt cell mitoses (Cii) versus constant crypt cell migration (Ciii) are illustrated. (Di) hierarchy of calcein-labelled live cells and propidium iodide (PI)-positive dead cells; (Dii) cells at the crypt opening are positive for activated caspase 3 and (Diii) the number of PI-positive shed cells increases over time in culture (see online supplementary movie S4). Significant differences were assessed by ANOVA followed by Tukey's post-hoc analysis; significant differences between pairs of mean values are indicated by linked dashed lines; *p<0.01. W=Wnt 3A, I=IGF-1, N=noggin, R=R-spondin-1, DKK-1=dikkopf-1.

In summary, we have developed a near-native human colonic crypt culture model. The functional interaction between morphogens and their relative influence of stem cell-driven tissue renewal reinforces the importance of the canonical Wnt signalling pathway. Future investigation of the modulators that establish morphogen gradients along the crypt-axis[16] and their influence on the efficiency of intestinal tissue renewal in health and disease promises novel insights into disease risk and prevention. The native colonic crypt model can also be used to investigate numerous other aspects of (patho)physiology including: membrane transport, microbial-epithelial interactions, mesenchymal-epithelial cell interactions, pharmacology and toxicology, in homeostasis and disease.

Acknowledgements The authors wish to thank Paul Thomas for bioimaging expertise, Andrew Loveday for technical assistance, Mohammad Abu-Elmagd for advice about in situ hybridisation, members of the Clark and Riley laboratories for quantitative reverse transcriptase polymerase chain reaction advice, Richard Evans-Gowing for expertise with H&E staining, and all the staff in the Gastroenterology Department and operating theatres at the Norfolk and Norwich University Hospital.

Contributors Data acquisition/analysis: AR, NW, AP, EM, AS, LB, AE-H, CK, AM, NO, WY. Material support: ML, CS, WS, RW, KS, RT, CJ, JH, SK, NO, WY. Study design: MRW, AR, AP, AM. Manuscript revision: All authors. Funding: MRW, AM, AS, ML. Paper authorship: MRW.

Funding The work was supported by BBSRC (BB/F015690/1, BB/D018196/1), the Boston Leukaemia and Cancer Research Fund, the Big C Appeal, the Humane Research Trust, and the John and Pamela Salter Trust.

Competing interests None.

Ethics approval East of England National Research Ethics Committee.

Provenance and peer review Not commissioned; externally peer reviewed.

Data sharing statement Unpublished data on crypt viability after 4 days, use of the alternative ALK inhibitor SB431542, suppression of LGR5-mRNA by DKK-1, IGF-1-stimulated crypt cell proliferation are available on request to the corresponding author.

REFERENCES

1 Snippert HJ, van der Flier LG, Sato T, *et al*. Intestinal crypt homeostasis results from neutral competition between symmetrically dividing Lgr5 stem cells. *Cell* 2010;143:134–44.
2 Lopez-Garcia C, Klein AM, Simons BD, *et al*. Intestinal stem cell replacement follows a pattern of neutral drift. *Science* 2010;330:822–5.
3 Scoville DH, Sato T, He XC, *et al*. Current view: intestinal stem cells and signaling. *Gastroenterology* 2008;134:849–64.
4 van der Flier LG, Clevers H. Stem cells, self-renewal, and differentiation in the intestinal epithelium. *Annu Rev Physiol* 2009;71:241–60.

5 van de Wetering M, Sancho E, Verweij C, *et al*. The beta-catenin/TCF-4 complex imposes a crypt progenitor phenotype on colorectal cancer cells. *Cell* 2002;111:241–50.
6 Kuhnert F, Davis CR, Wang HT, *et al*. Essential requirement for Wnt signaling in proliferation of adult small intestine and colon revealed by adenoviral expression of Dickkopf-1. *Proc Natl Acad Sci USA* 2004;101:266–71.
7 Pinto D, Gregorieff A, Begthel H, *et al*. Canonical Wnt signals are essential for homeostasis of the intestinal epithelium. *Genes Dev* 2003;17:1709–13.
8 Barker N, van Es JH, Kuipers J, *et al*. Identification of stem cells in small intestine and colon by marker gene Lgr5. *Nature* 2007;449:1003–7.
9 Zhao J, de Vera J, Narushima S, *et al*. R-spondin1, a novel intestinotrophic mitogen, ameliorates experimental colitis in mice. *Gastroenterology* 2007;132:1331–43.
10 de Lau W, Barker N, Low TY, *et al*. Lgr5 homologues associate with Wnt receptors and mediate R-spondin signalling. *Nature* 2011;476:293–7.
11 Carmon KS, Gong X, Lin Q, *et al*. R-spondins function as ligands of the orphan receptors LGR4 and LGR5 to regulate Wnt/beta-catenin signaling. *Proc Natl Acad Sci USA* 2011;108:11452–7.
12 Haramis AP, Begthel H, van den Born M, *et al*. De novo crypt formation and juvenile polyposis on BMP inhibition in mouse intestine. *Science* 2004;303:1684–6.
13 Hardwick JC, Van Den Brink GR, Bleuming SA, *et al*. Bone morphogenetic protein 2 is expressed by, and acts upon, mature epithelial cells in the colon. *Gastroenterology* 2004;126:111–21.
14 He XC, Zhang J, Tong WG, *et al*. BMP signaling inhibits intestinal stem cell self-renewal through suppression of Wnt-beta-catenin signaling. *Nat Genet* 2004;36:1117–21.
15 Freeman TJ, Smith JJ, Chen X, *et al*. Smad4-mediated signaling inhibits intestinal neoplasia by inhibiting expression of beta-catenin. *Gastroenterology* 2012;142:562–71 e2.
16 Kosinski C, Li VS, Chan AS, *et al*. Gene expression patterns of human colon tops and basal crypts and BMP antagonists as intestinal stem cell niche factors. *Proc Natl Acad Sci USA* 2007;104:15418–23.
17 Zhou XP, Woodford-Richens K, Lehtonen R, *et al*. Germline mutations in BMPR1A/ALK3 cause a subset of cases of juvenile polyposis syndrome and of Cowden and Bannayan-Riley-Ruvalcaba syndromes. *Am J Hum Genet* 2001;69:704–11.
18 Howe JR, Roth S, Ringold JC, *et al*. Mutations in the SMAD4/DPC4 gene in juvenile polyposis. *Science* 1998;280:1086–8.
19 Howe JR, Bair JL, Sayed MG, *et al*. Germline mutations of the gene encoding bone morphogenetic protein receptor 1A in juvenile polyposis. *Nat Genet* 2001;28:184–7.
20 Sato T, Stange DE, Ferrante M, *et al*. Long-term expansion of epithelial organoids from human colon, adenoma, adenocarcinoma, and Barrett's epithelium. *Gastroenterology* 2011;141:1762–72.
21 Jung P, Sato T, Merlos-Suarez A, *et al*. Isolation and in vitro expansion of human colonic stem cells. *Nat Med* 2011;17:1225–7.
22 Yui S, Nakamura T, Sato T, *et al*. Functional engraftment of colon epithelium expanded in vitro from a single adult Lgr5(+) stem cell. *Nat Med* 2012;18:618–23.
23 Reynolds A, Parris A, Evans LA, *et al*. Dynamic and differential regulation of NKCC1 by calcium and cAMP in the native human colonic epithelium. *J Physiol* 2007;582:507–24.
24 Lindqvist S, Hernon J, Sharp P, *et al*. The colon-selective spasmolytic otilonium bromide inhibits muscarinic M(3) receptor-coupled calcium signals in isolated human colonic crypts. *Br J Pharmacol* 2002;137:1134–42.
25 Oue N, Sentani K, Noguchi T, *et al*. Serum olfactomedin 4 (GW112, hGC-1) in combination with Reg IV is a highly sensitive biomarker for gastric cancer patients. *Int J Cancer* 2009;125:2383–92.
26 Miyoshi H, Ajima R, Luo CT, *et al*. Wnt5a potentiates TGF-beta signaling to promote colonic crypt regeneration after tissue injury. *Science* 2012;338:108–13.
27 Sato T, Vries RG, Snippert HJ, *et al*. Single Lgr5 stem cells build crypt-villus structures in vitro without a mesenchymal niche. *Nature* 2009;459:262–5.
28 Simmons JG, Ling Y, Wilkins H, *et al*. Cell-specific effects of insulin receptor substrate-1 deficiency on normal and IGF-I-mediated colon growth. *Am J Physiol Gastrointest Liver Physiol* 2007;293:G995–1003.
29 VanDussen KL, Carulli AJ, Keeley TM, *et al*. Notch signaling modulates proliferation and differentiation of intestinal crypt base columnar stem cells. *Development* 2012;139:488–97.
30 Munoz J, Stange DE, Schepers AG, *et al*. The Lgr5 intestinal stem cell signature: robust expression of proposed quiescent '+4' cell markers. *EMBO J* 2012;31:3079–91.
31 van der Flier LG, Haegebarth A, Stange DE, *et al*. OLFM4 is a robust marker for stem cells in human intestine and marks a subset of colorectal cancer cells. *Gastroenterology* 2009;137:15–17.
32 Sato T, van Es JH, Snippert HJ, *et al*. Paneth cells constitute the niche for Lgr5 stem cells in intestinal crypts. *Nature* 2011;469:415–18.
33 Ziskin JL, Dunlap D, Yaylaoglu M, *et al*. In situ validation of an intestinal stem cell signature in colorectal cancer. *Gut* 2012;62:1012–23.
34 van Es JH, Sato T, van de Wetering M, *et al*. Dll1(+) secretory progenitor cells revert to stem cells upon crypt damage. *Nat Cell Biol* 2012;14:1099–104.
35 Medema JP, Vermeulen L. Microenvironmental regulation of stem cells in intestinal homeostasis and cancer. *Nature* 2011;474:318–26.
36 Kaur P, Potten CS. Cell migration velocities in the crypts of the small intestine after cytotoxic insult are not dependent on mitotic activity. *Cell Tissue Kinet* 1986;19:601–10.
37 Playford MP, Bicknell D, Bodmer WF, *et al*. Insulin-like growth factor 1 regulates the location, stability, and transcriptional activity of beta-catenin. *Proc Natl Acad Sci U S A* 2000;97:12103–8.
38 Chen B, Dodge ME, Tang W, *et al*. Small molecule-mediated disruption of Wnt-dependent signaling in tissue regeneration and cancer. *Nat Chem Biol* 2009;5:100–7.
39 Farin HF, Van Es JH, Clevers H. Redundant Sources of Wnt Regulate Intestinal Stem Cells and Promote Formation of Paneth Cells. *Gastroenterology* 2012;143:1518–29.
40 Leedham SJ, Rodenas-Cuadrado P, Howarth K, *et al*. A basal gradient of Wnt and stem-cell number influences regional tumour distribution in human and mouse intestinal tracts. *Gut* 2012;62:83–93.
41 Suzuki H, Watkins DN, Jair KW, *et al*. Epigenetic inactivation of SFRP genes allows constitutive WNT signaling in colorectal cancer. *Nat Genet* 2004;36:417–22.
42 Belshaw NJ, Pal N, Tapp HS, *et al*. Patterns of DNA methylation in individual colonic crypts reveal aging and cancer-related field defects in the morphologically normal mucosa. *Carcinogenesis* 2010;31:1158–63.
43 Furukawa K, Sato T, Katsuno T, *et al*. Smad3 contributes to positioning of proliferating cells in colonic crypts by inducing EphB receptor protein expression. *Biochem Biophys Res Commun* 2011;405:521–6.
44 Farrall AL, Riemer P, Leushacke M, *et al*. Wnt and BMP signals control intestinal adenoma cell fates. *Int J Cancer* 2012;131:2242–52.

SUPPLEMENTARY INFORMATION

Supplementary Methods

Reagents. Human colonic crypt culture media and supplements: Advanced F12/DMEM, B27 and N2 were all from Invitrogen. Small molecule inhibitors were: A83-01 (Tocris), DMH-1 (Tocris) and IWP2 (Sigma). Growth factor-reduced Matrigel was purchased from BD Bioscience. Human recombinant growth factors used for colonic crypt culture experiments were: IGF-1 (Sigma); R-spondin-1 (Sino Biological or R&D Systems); Wnt 3A (R&D systems), Gremlin-1 (R&D Systems); Noggin (Peprotech); TGFβ-1 (R&D systems), BMP4 (Peprotech), EGF (Sigma) and DKK-1 (R&D Systems).

Immunolabelling of native and cultured colonic crypts was performed using the following antibodies: mouse anti-β-catenin (BD Bioscience), mouse anti-dephospho-beta catenin (Upstate), goat anti-E-cadherin (R&D Systems), mouse anti-LGR5 (Origene), mouse anti-OLFM4 [1], rabbit anti-OLFM4 (Abcam), rabbit anti-Axin-2 (Abcam), anti-active-caspase 3 (Cell Signalling), mouse anti-Ki67 antibody (Dako), rat anti-BrdU (Abcam), anti-phospho-SMAD1,5,8 (Cell Signalling), anti-phospho-SMAD2,3 (Cell Signalling), rabbit anti-Wnt-3A (Abcam), goat anti-GFP (Abcam) and goat anti-FITC (Abcam).

Human colonic crypt isolation and culture. Colonic crypts were isolated as described previously [2 3]. Fresh mucosal tissue samples were collected in ice cold PBS, transported to the laboratory and incubated in Hepes-buffered saline (HBS): (mM) NaCl 140, KCl 5, Hepes (N-2-hydroxyethylpiperazine-N2-ethanesulphonic acid) 10, d-glucose 5.5, Na2HPO4 1, MgCl2 0.5, CaCl2 1, and placed in HBS, which was devoid of both Ca^{2+} and Mg^{2+}, and supplemented with EDTA (diaminoethanetetraacetic acid disodium salt) (1mM), for 1 h at room temperature. Crypts were liberated by serial rounds of vigorous shaking, crypt sedimentation and collection. Sedimented crypts were collected and mixed in Matrigel and a 20 μl droplet containing 50-100 crypts was placed onto no. 0 glass coverslips (VWR) contained within a 12 well plate. After polymerisation at 37^0C for 5-10 mins, crypts were flooded with 0.5 mls of human colonic crypt culture medium (hCCCM), a variant of that described recently for human intestinal stem cell/organoid culture[4 5]: advanced F12/DMEM containing B27, N2, n-acetylcysteine (1 mM), hepes (10 mM), penicillin/ streptomycin (100 U/ml), L-Glutamine (2mM), Wnt-3A (100 ng/ml), IGF-1 (50 ng/ml), Noggin (100 ng/ml) or Gremlin-1 (200 ng/ml), RSPO-1 (500 ng/ml), and the ALK 4/5/7 inhibitor A83-01-01 (0.5 μM). hCCCM was changed every two days and was modified further according to the stated experimental conditions. BrdU (10 μM) was added to the experimental crypt culture media as described to monitor crypt cell proliferation and migration. Propidium iodide (1 μg/ml) and calcein (5 μM) were added to the medium for visualisation of live/dead crypt cells.

Whole mount immunohistochemistry. Following embedding in Matrigel, microdissected-native crypts or cultured-crypts were fixed with 4% PFA for 1 hour and permeabilized with either SDS (1%) or Triton X-100 (0.5% w/v PBS, 30 min). Non-specific binding sites were blocked with 10% goat and/or donkey serum and 1% bovine serum albumin for 2 h and washed with PBS. Crypts were incubated with primary antibodies (1:100-200 dilution) overnight at 4^oC. Immmunolabelling was visualised by using an appropriate combination of species-specific Alexafluor-conjugated secondary antibodies (488, 568, and 647 nm) raised in donkey and/or goat (Invitrogen). Crypts were mounted on glass slides with Vectashield containing DAPI (Vector labs).

Dual whole mount mRNA *in situ* hybridisation and immunohistochemistry. High affinity ~20'mer locked nucleic acid (LNA), FAM-conjugated probes were used in combination with high stringent hybridisation and washing to label *LGR5* mRNA. The processing for *in situ* hybridisation was modified from that described previously [6]. Briefly, microdissected-native crypts embedded in Matrigel were fixed with 4% PFA and washed with PBS-T (0.1% Tween-20). Crypts were then treated with HCl-PBST (0.2 N) followed by Proteinase K (10 μg/ml, Sigma) and post-fixed with PFA (4%) for 10 mins. After a PBST wash, crypts were incubated in a mix of probe (40 nM), denatured salmon sperm (50 μl/ml, Sigma) and hybridisation buffer (formamide,50%; 1.3xSSC; CHAPS, 0.5%; Tween-20, 0.2%; EDTA, 5 mM; in DEPC H_20) for 14 hours at the hybridisation temperature specified for the probe (Exiqon). Crypts were treated with x5 SSC for 10 mins followed by 0.2% SSC for 1 hour. A 1 hour block with BBM (Roche) preceded addition of the primary antibodies: goat anti-FITC, mouse anti-OLFM4 and rabbit anti-E-cadherin (all at 1:100 dilution). The next day, secondary antibodies were added as described for the immunohistochemistry procedure. The custom LNA probe sequence used for *LGR5* was*:* /5'-FAM/ATGAGGAAGCAAAGGGAATTGAGC /3'-FAM/. Hybridisation specificity was confirmed by use of a positive control β-actin LNA-probe and a negative control scrambled LNA-probe (both Exiqon).

RNA isolation Freshly isolated or cultured crypts were pelleted and placed in RNA later (Ambion). RNA was extracted using the RNeasy mini kit (Qiagen). cDNA was generated using the Superscript (II) RT kit (Invitrogen).

RT-PCR was performed using the BioTAQ PCR kit (Bioline) with a G-Storm thermal cycler (GRI). After 30 cycles the PCR products were run on a 1% agarose gel visualised by ethidium bromide staining. The forward and reverse primers for Wnt3A were:

Gene	Forward Primer	Reverse Primer	Product (base pairs)
Wnt3A	ctgctcagctgcgccccttcttt	ttcagcggcctccccattcattcc	404

Measurement of gene expression by quantitative RT-PCR. qRTPCR was performed using KAPA Universal Probe qPCR kit (Primer Design) following manufacturer's instructions. YWHAZ was used to normalize expression. ΔcT values were generated for each sample and relative ΔΔcT values are presented. Primers are available on request.

Supplementary References

45. **Oue N,** Sentani K, Noguchi T, et al. Serum olfactomedin 4 (GW112, hGC-1) in combination with Reg IV is a highly sensitive biomarker for gastric cancer patients. *Int J Cancer* 2009;**125**:2383-92.
46. **Sweetman D,** Goljanek K, Rathjen T, et al. Specific requirements of MRFs for the expression of muscle specific microRNAs, miR-1, miR-206 and miR-133. *Dev Biol* 2008;**321**:491-9.

Supplementary Figure 1: Intestinal stem/progenitor cell status in native human colonic crypts. (A) Schematic representation of immunofluoresence images of human colonic crypt-base; crypt cell types were identified according to congruent expression of stem cell markers OLFM4 and LGR5, crypt cell (nuclear) morphology and comparison with dual immuno/*in situ* hybridisation fluorescence labelling of muc2/lgr5-mRNA, as shown in (B). (C) Double immunofluorescence labelling of OLFM4 and Ki-67 to assess the proliferative status of intestinal stem/progenitor cells, accompanying analysis is presented in the main Figure 1F. (D) Spatial correlation of mitogenic Wnt signals (i.e. nuclear beta catenin) and target gene expression (i.e. c-MYC) in the stem cell niche located at the human colonic crypt-base; images complement data presented in the main Figure 2. Scale bar = (A, D) 50 mm, (C) 20 mm; DIC – differential interference contrast; E-CAD – e-cadherin.

Supplementary Figure 2: **Dual fluorescence mRNA *in situ* hybridisation and immunolabelling along the native human colonic crypt-axis.** (A) example of congruent expression for lgr5-mRNA and OLFM4-protein by slender cells interspersed between goblet-like cells at the native human colonic crypt-base (*cf.* main Figure 1C and supplementary Figure 1B). (B) a corresponding negative control for fluorescence *in situ* hybridisation using a scrambled oligonucleotide probe in conjunction with OLFM4-immunolabelling; the crypt was obtained from the same sample as in (A) and the processing conditions and acquisition settings were identical. (D) positive control for fluorescence *in situ* hybridisation using an antisense oligonucleotide probe specific for beta actin-mRNA, note labelling along the entire crypt axis compared to lgr5-mRNA which is only located at the crypt-base (*cf.* main Figure 1C). DIC – differential interference contrast; E-CAD – e-cadherin.

Supplementary Figure 3: Immunolabelling of distinct cell types within native human colonic crypts. (A) The enterocyte marker FABP1 is predominantly expressed by columnar enterocytes located towards the top of the crypt. A monoclonal MUC-2 antibody marks perinuclear nascent protein in cells with a goblet-like morphology (A), while labelling with a MUC-2 polyclonal antibody is more prominent throughout the cytoplasm of goblet cells (B), which are interspersed with distinct, slender OLFM4-positive cells. (C) Relatively rare chromogranin A (CGA)-positive enteroendocrine cells intermingle between goblet-like cells and slender OLFM4-positive cells. (D) Recently characterised tuft cells are visualised by immunolabelling COX-1 and are typically elliptical with a nucleus indented from the basal pole. These immunolabelling patterns are reproduced in cultured human colonic crypts (see main Figure 6H). Scale bar = (A) 50 μm, (B) 30 μm.

Supplementary Figure 4: Comparative histology of native versus cultured human colonic crypts.

Fixed biopsy samples (A) and cultured human colonic crypts (day 4) (B) were processed for haematoxylin and eosin staining. Cultured colonic crypts exhibit similar topology, polarity and morphology to native colonic crypts, but are not surrounded by sub-epithelial mesenchymal cell types. (C) Microdissected (i.e. native) and (D) cultured human colonic crypts were processed for immunolabelling of smooth muscle actin, a marker of sub-epithelial myofibroblasts. Scale bar = 50 μm

Supplementary Figure 5: Inhibition of Wnt signals or activation of TGFβ/BMP signals compromises cultured human colonic crypt morphology

(A) The contribution of RSPO1/Wnt3A to the maintenance of crypt length (*cf.* main Figure 3C) is suppressed by the canonical Wnt pathway inhibitor DKK-1 (800 ng/ml). (B) BMP (100 ng/ml) treatment compromises crypt length and morphology and this is abrogated by noggin (100/ng/ml); similarly the adverse effects of TGF beta (20 ng/ml) are prevented by the ALK4/5/7 inhibitor, A83-01 (0.5 μM). Crypts were cultured for three days under the indicated conditions. In each experiment, crypts were derived from N≥2 subjects, with n ≥ 4 crypts in each experimental group. The control culture conditions were: (A) = ADF12/B27/N2/nAC/IGF1 (50 ng/ml)/Gremlin1 (200 ng/ml);
(B) = ADF12/B27/N2/nAC/IGF1 (50 ng/ml)/Wnt3A (100 ng/ml)/RSPO1 (500 ng/ml) /A83-01 (0.5 μM);
(C) = ADF12/B27/N2/nAC/IGF1 (50 ng/ml)/Wnt3A (100 ng/ml)/RSPO1 (500 ng/ml)/Noggin (100 ng/ml). Significant differences between pairs of mean values are indicated by linked blue lines ($p<0.05$); ADF12 – advanced DMEM/F12; nAC – n-acetylcysteine

Supplementary Figure 6: Effects of EGF on cultured human colonic crypt morphology

Replacement of IGF-1 with EGF (50 ng/ml) in the colonic crypt culture media induced re-modelling of human colonic crypt morphology into a typical budding organoid configuration over a 6-day culture period. D1, D3 and D6 indicate number of days in culture; dashed white lines indicate lumen of original crypt; dashed black lines indicate zoomed regions containing a crypt domain budding from the original isolated crypt; scale bar – 50 μm

Supplementary Figure 7: Wnt, TGFβ and BMP signalling gradients are maintained along the cultured human colonic crypt-axis.

Crypts were cultured for 4 days and processed for axin-2, p-SMAD2,3 or p-SMAD1,5,8 immunolabelling. Confocal microscopy using optimised acquisition settings for each label revealed an immunofluorescence gradient that predominated at the crypt-base for axin2 and at the crypt-top for p-SMAD1,5,8, while the labelling was highest in the mid-crypt region for p-SMAD2,3. These patterns recapitulated those observed in native crypts (*c.f.* Figure 2 in the main paper). Colonic crypt culture: Wnt 3A (100 ng/m), IGF1 (50 ng/ml), Noggin (100 ng/ml), R-spondin-1 (500 ng/ml), A83-01 (0.5 μM).

Supplementary Figure 8: Expression profile for several marker genes is similar for native and cultured human colonic crypts crypts.

RNA was extracted from freshly isolated human colonic crypts and from crypts cultured for 3 days. Expression of stem cell-, proliferation- and differentiation-markers was analysed by qRT-PCR. Data are presented as relative changes in gene expression between freshly isolated and colonic crypts cultured in the presence and absence of noggin. The presence of noggin maintains LGR5 and OLFM4 expression albeit at apparently reduced levels, while ID2 gene expression is downregulated. One

caveat to bear in mind when making this comparison is that mRNA levels in freshly isolated crypts may be subject to stress induced change during the isolation procedure. Colonic crypt culture: Wnt 3A (100 ng/m), IGF1 (50 ng/ml), Noggin (100 ng/ml), R-spondin-1 (500 ng/ml), A83-01 (0.5 μM).

Supplementary Table 1: Comparative characteristics/parameters of native versus cultured human colonic crypts

Characteristic/Parameter	**Native human colonic crypts**	**Cultured human colonic crypts**	**Data source**
% Stem/Progenitor cells at crypt-base (% proliferating SP cells)	50 (50)	40 (40)	Figs 1E and 6F (Figs 1F and 6G)
Crypt cell proliferation (% $Ki67^+$) Base-,Mid-,Upper-crypt	 55,45,20	 55;30;10	 Figs 1B and 6A, 7B, 7D
% stem:% goblet:% other cell types Crypt-base Mid-crypt Upper-crypt	 50:30:20 15:45:40 5:40:55	 40:30:30 15:30:55 5:30:65	 Figs 1E and 6D, 6F, 6I
Presence of enterocytes, enteroendocrine and tuft cells	YES	YES	Supplementary Fig. 3 and main Fig. 6H
Wnt signalling gradient (Nuclear beta catenin & nuclear axin2)	High-to-low from crypt-base	High-to-low from crypt-base	Figs 2A, 2B and Figs 4A-D
BMP/p-SMAD 1,5,8 gradient	High-to-low from crypt surface	High-to-low from crypt surface	Figs 2D and Supplementary Fig. 5
TGFβ/p-SMAD 2,3 profile	Higher in mid-crypt	Higher in mid-crypt	Figs 2C and Supplementary Fig. 7
Cell apoptosis/death/shedding Crypt base Crypt top/surface epithelium	 <0.5% (caspase 3^+) Cell shedding	 <0.5% (caspase $3^+/PI^+$) Cell Shedding	 Data not shown; Fig. 8D Data not shown; Fig. 8D

Supplementary Movie 1

3D reconstruction of confocal image stack of LGR5/OLFM4/E-CAD immunolabelling

Supplementary Movie 2

Timelapse movie of colonic crypt proliferation and migration (x20 objective)

Supplementary Movie 3

Timelapse movie of colonic crypt proliferation (x63 objective)

Supplementary Movie 4

Timelapse movie of detachment-induced cell death following shedding from the surface epithelium. Loss of cell viability was visualised by intense red bursts of fluorescence associated with propidium iodide binding to cell nuclei following rupture of cell membranes.

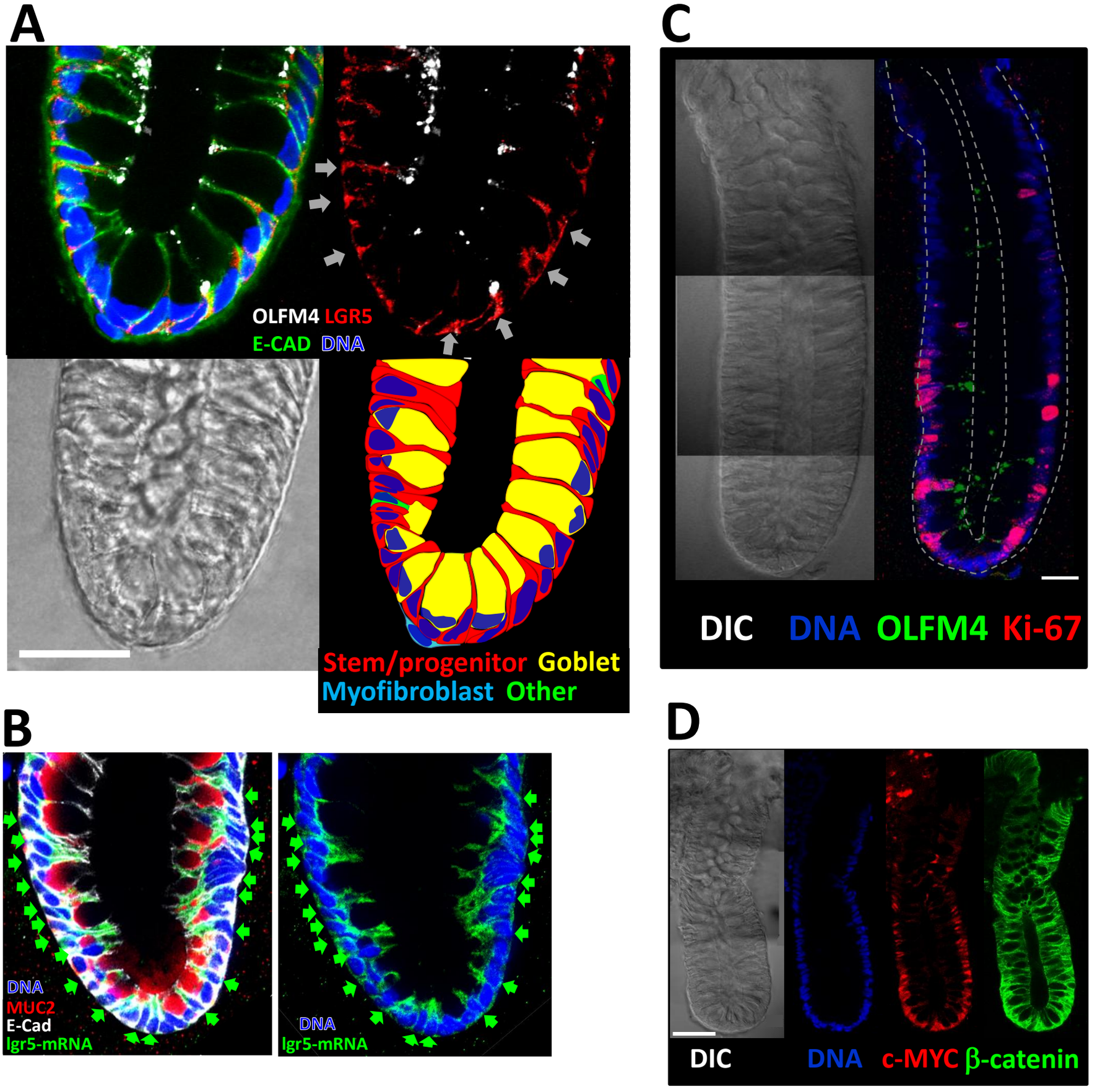

Supplementary Figure 1

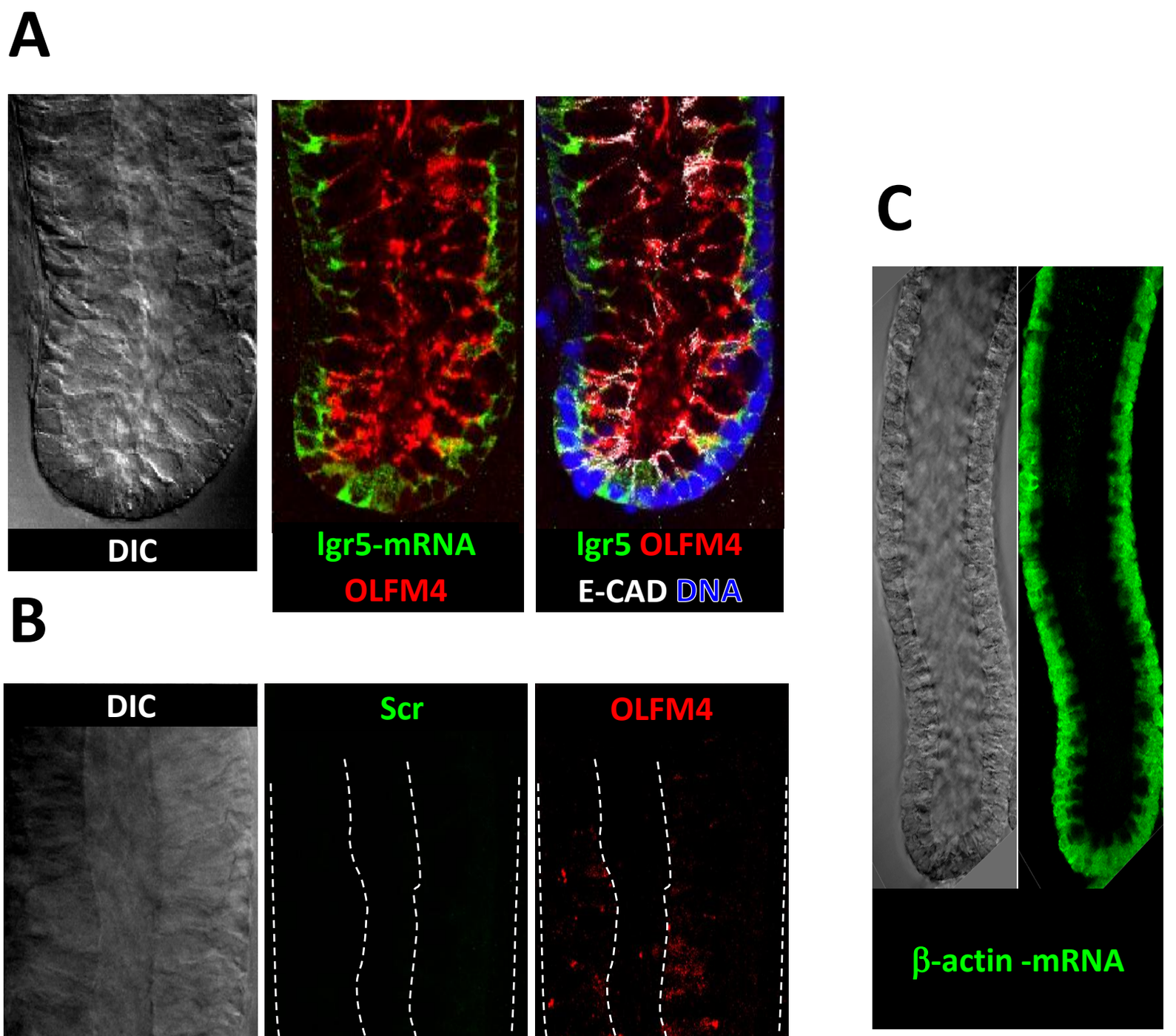

Supplementary Figure 2

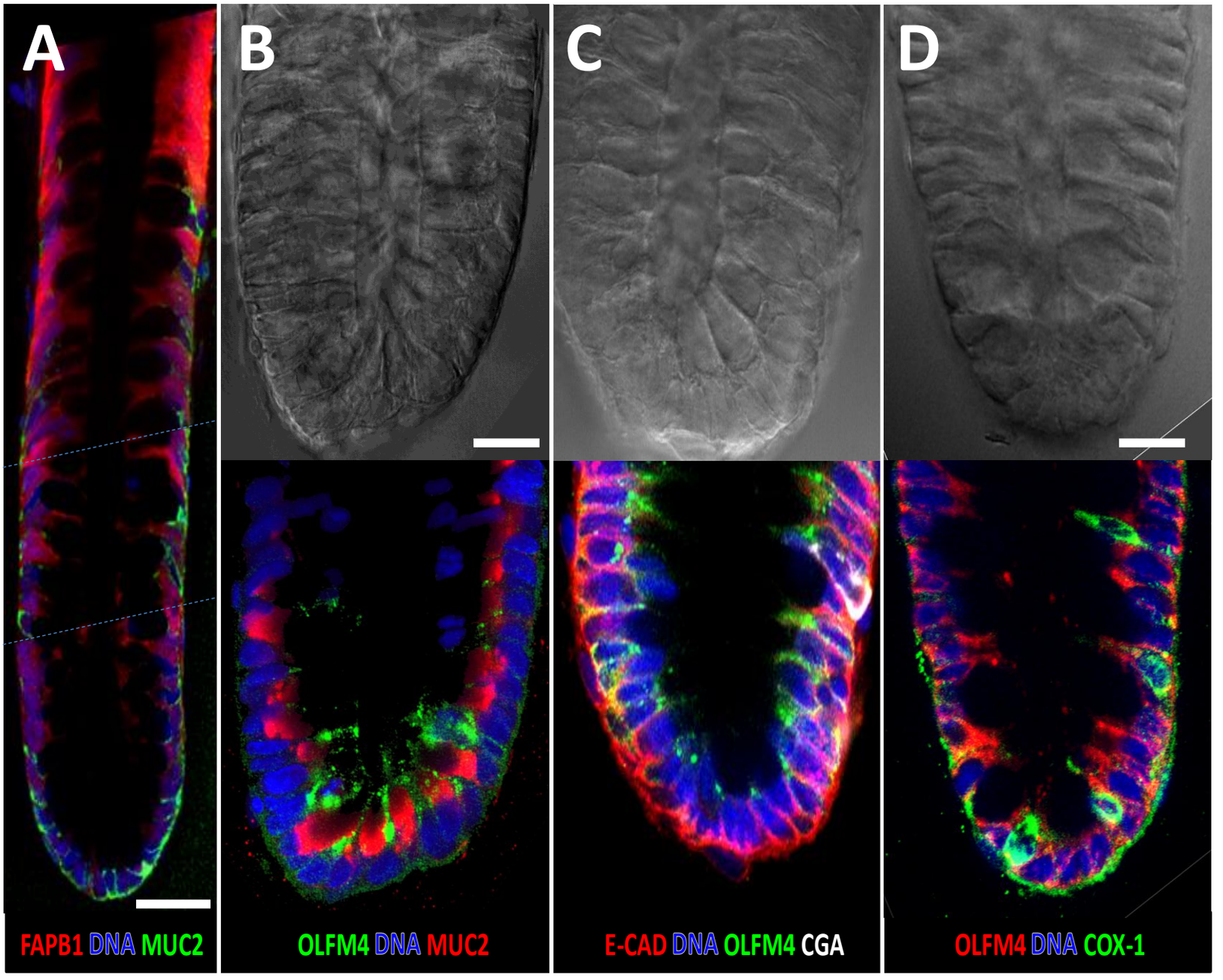

Supplementary Figure 3

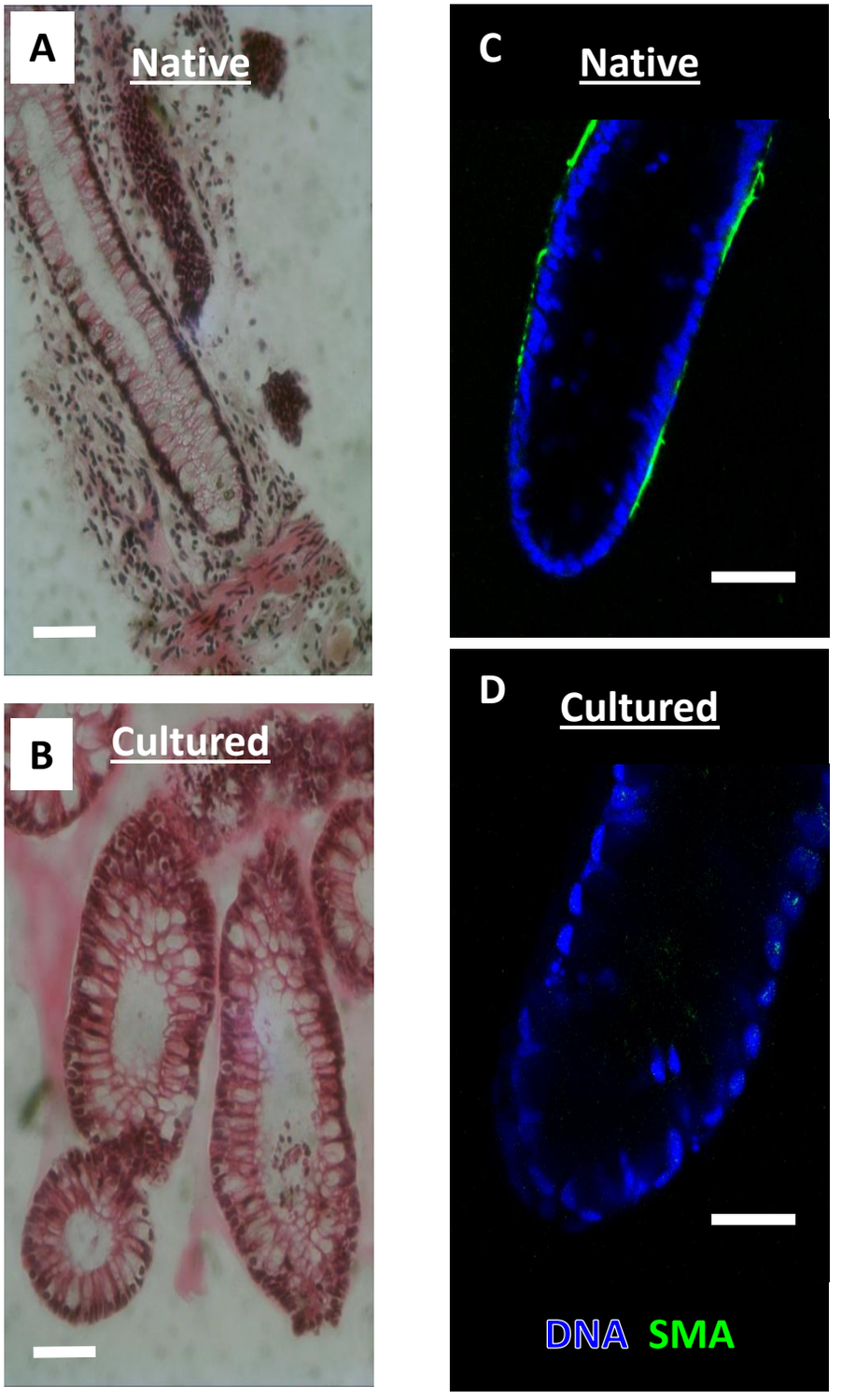

Supplementary Figure 4

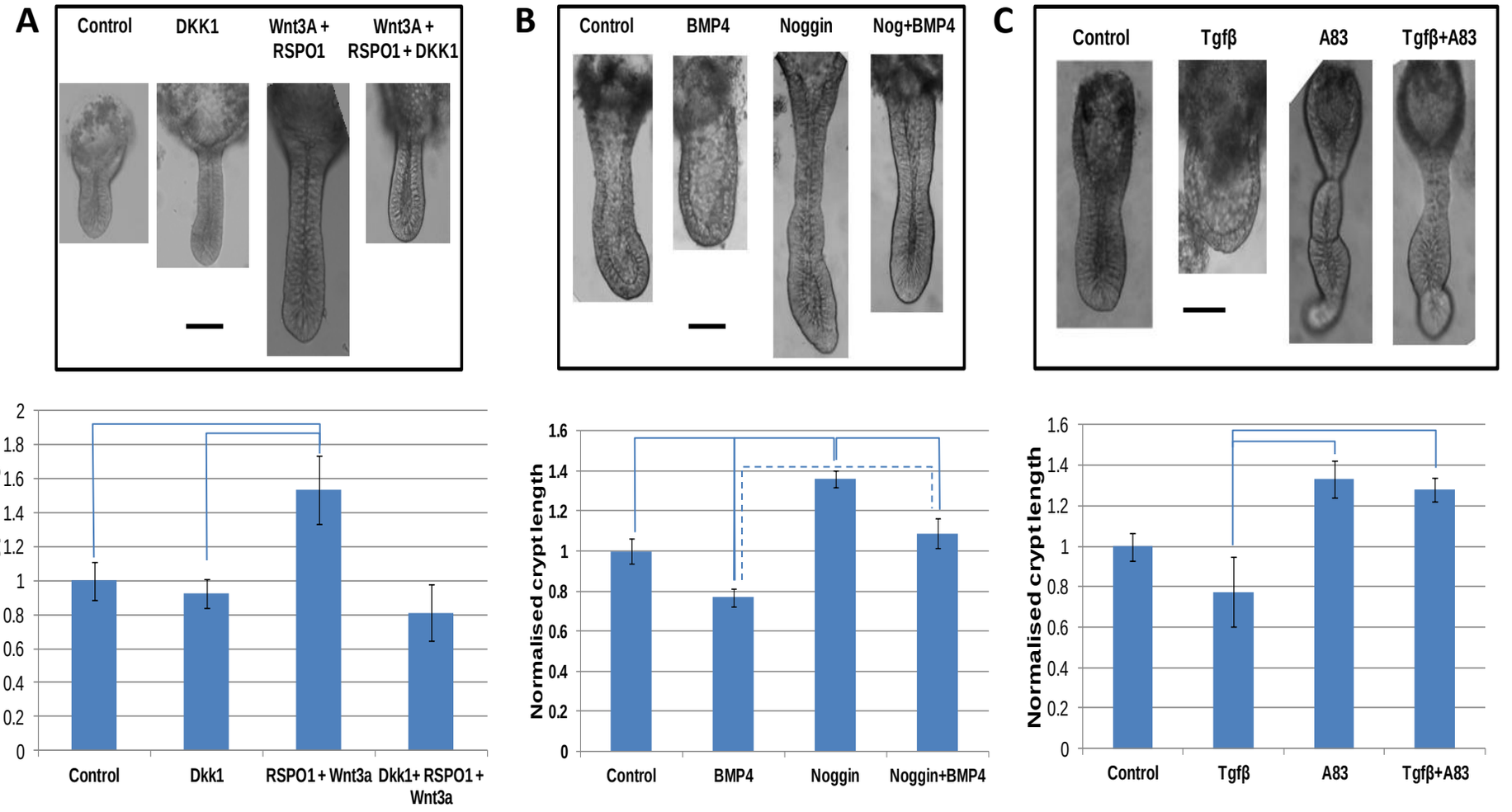

Supplementary Figure 5

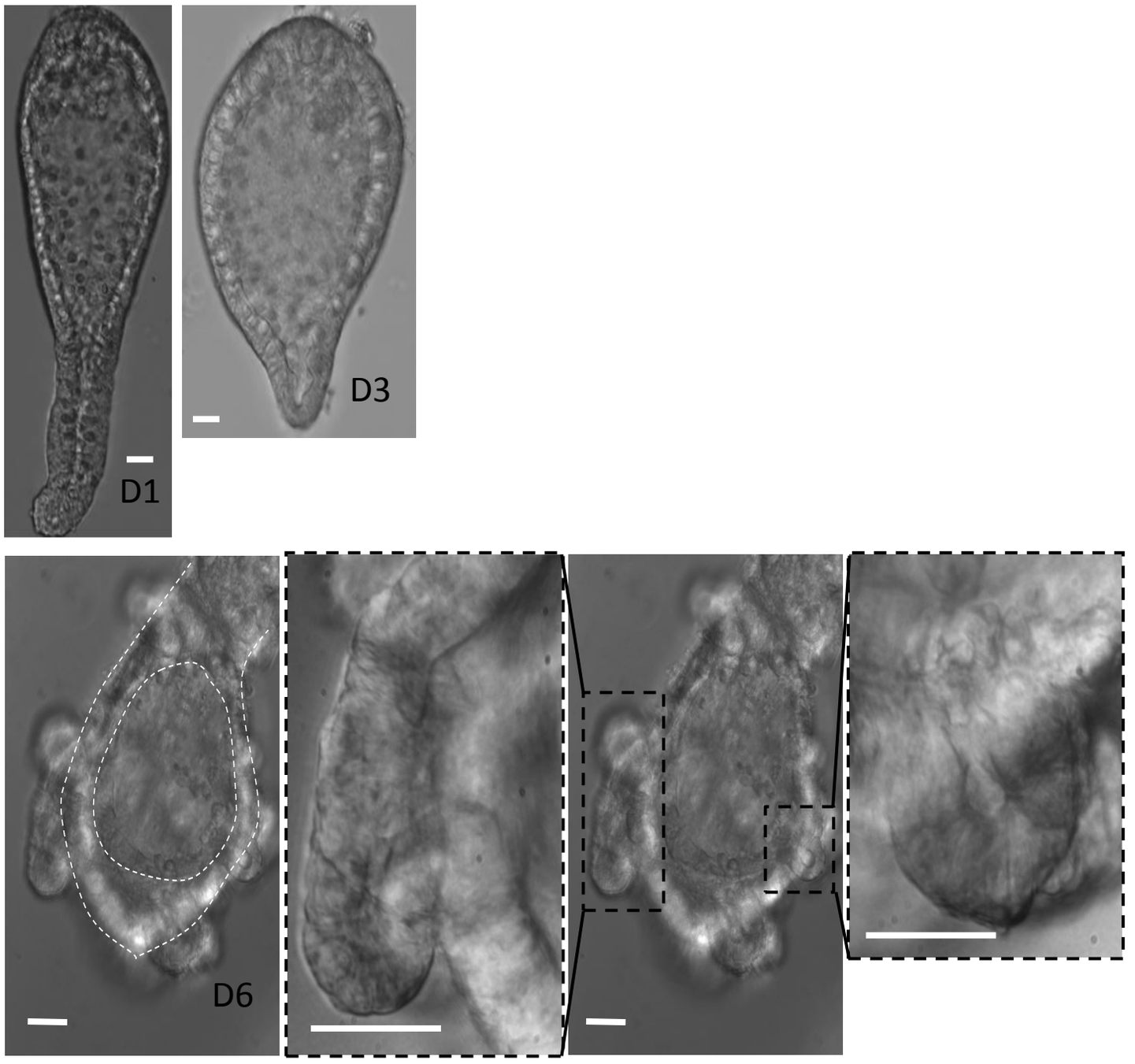

Supplementary Figure 6

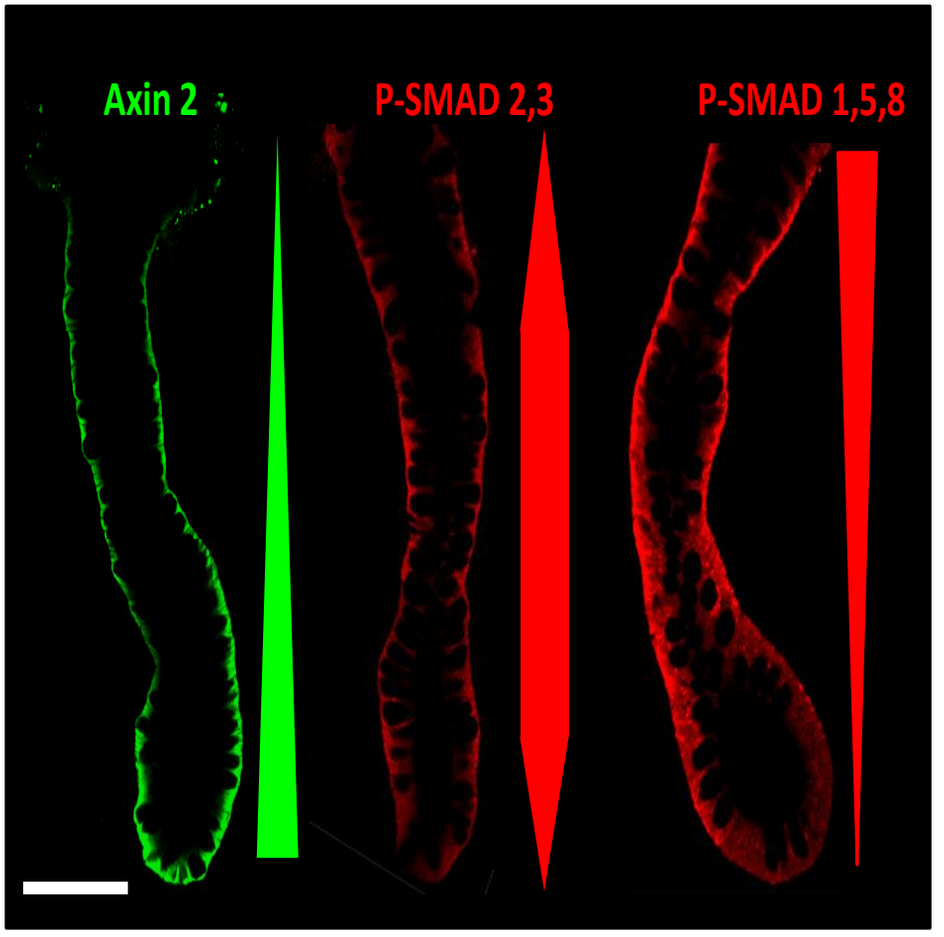

Supplementary Figure 7

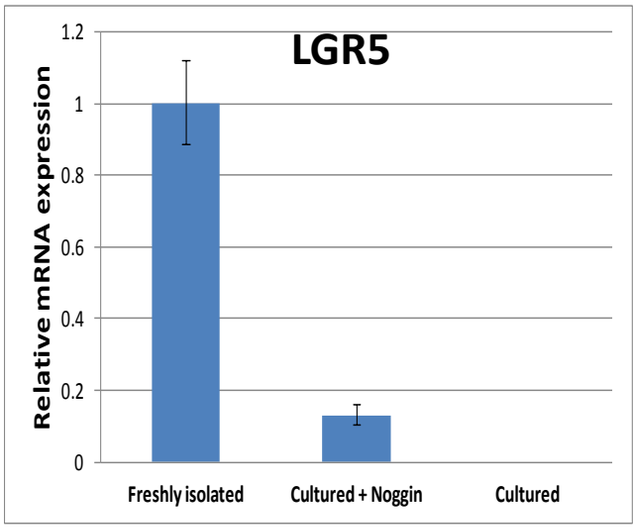

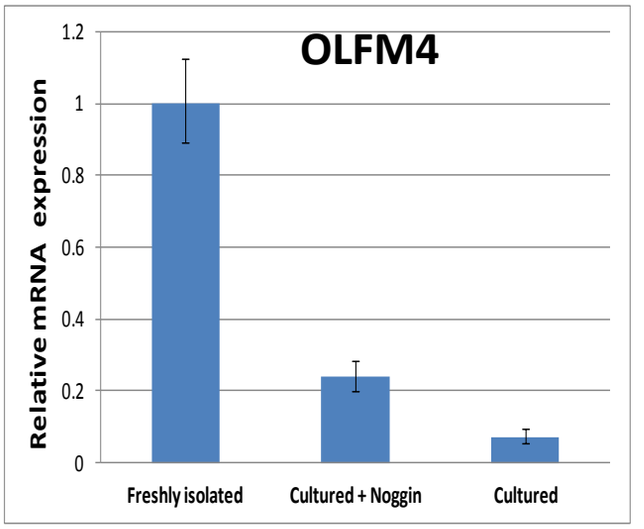

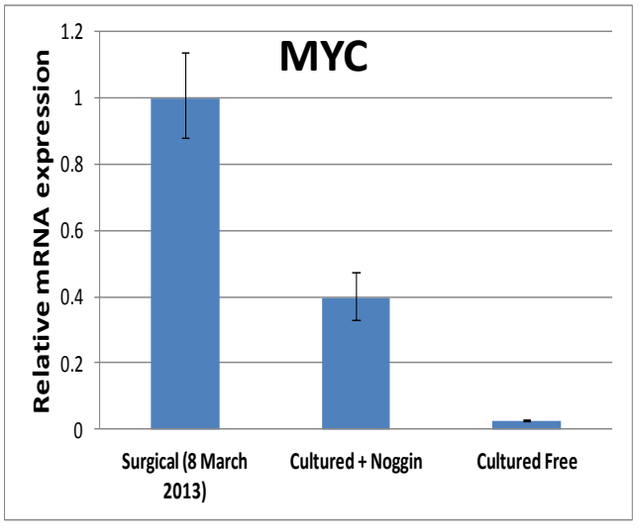

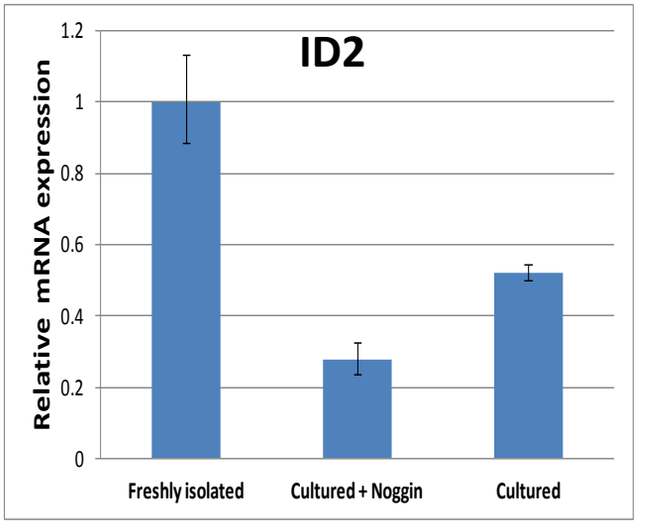

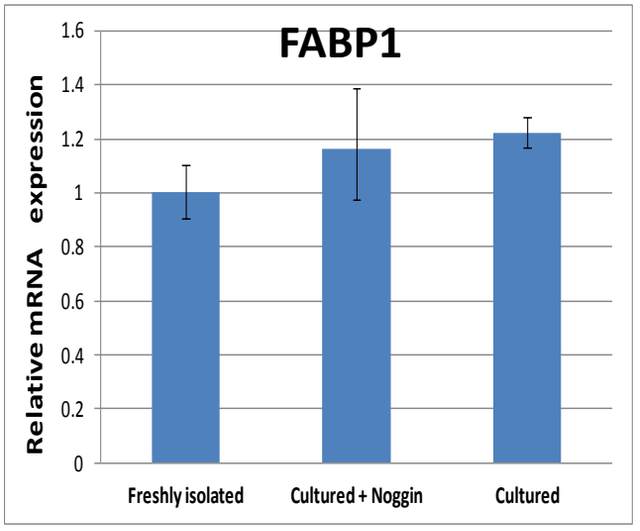

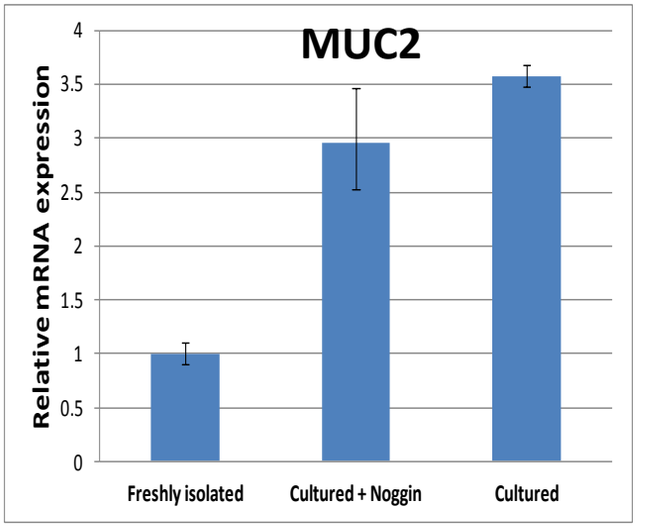

Supplementary Figure 8